

Bohr Hamiltonian with deformation-dependent mass term for the Kratzer potential

Dennis Bonatsos¹, P. E. Georgoudis¹, N. Minkov², D. Petrellis¹, and C. Quesne³

¹*Institute of Nuclear and Particle Physics, National Centre for Scientific Research "Demokritos", GR-15310 Aghia Paraskevi, Attiki, Greece*

²*Institute of Nuclear Research and Nuclear Energy, Bulgarian Academy of Sciences, 72 Tzarigrad Road, 1784 Sofia, Bulgaria and*

³*Physique Nucléaire Théorique et Physique Mathématique, Université Libre de Bruxelles, Campus de la Plaine CP229, Boulevard du Triomphe, B-1050 Brussels, Belgium*

The Deformation Dependent Mass (DDM) Kratzer model is constructed by considering the Kratzer potential in a Bohr Hamiltonian, in which the mass is allowed to depend on the nuclear deformation, and solving it by using techniques of supersymmetric quantum mechanics (SUSYQM), involving a deformed shape invariance condition. Analytical expressions for spectra and wave functions are derived for separable potentials in the cases of γ -unstable nuclei, axially symmetric prolate deformed nuclei, and triaxial nuclei, implementing the usual approximations in each case. Spectra and $B(E2)$ transition rates are compared to experimental data. The dependence of the mass on the deformation, dictated by SUSYQM for the potential used, moderates the increase of the moment of inertia with deformation, removing a main drawback of the model.

I. INTRODUCTION

In the non-relativistic Schrödinger equation usually the mass is assumed to be independent of position. However, there are certain physical systems in which, according to the experimental data, the effective mass should be position dependent. Apart from semiconductor theory, in which effective masses depending on the spatial coordinates have been used since many years [1–6], this is also the case in atomic nuclei, especially in the collective model of Bohr [7].

If the mass is position dependent, then it does not commute with the momentum. Therefore there are many ways to generalize the usual form of the kinetic energy in order to obtain a Hermitian operator. In Ref. [5], the most general non-relativistic Schrödinger equation which possesses a position dependent mass and at the same time respects hermiticity was proposed. A further step was taken in Refs. [8, 9], in which a general scheme was proposed, through the introduction of a parameter a in the kinetic energy term, which apart from hermiticity also ensures the exact solvability of the relevant non-relativistic Schrödinger equation, in which the mass dependence on the position is reflected in the parameter a .

In the realm of nuclear physics, the need for three different mass coefficients in the low lying collective bands of well-deformed axially symmetric even-even nuclei has been demonstrated using the experimental data for spectra and $B(E2)$ transition rates by Jolos and von Brentano [10–12]. In an extended version of this approach [13, 14] a mass tensor with deformation dependent components is introduced, the method being applicable to nuclei of arbitrary shape. This approach has been recently extended to odd nuclei [15, 16].

It has been recently proved [17] that by allowing the nuclear mass to depend on the deformation, the rate of increase of the moment of inertia with deformation is moderated, thus removing a main drawback [18] of the

Bohr Hamiltonian [7]. This has been achieved by using a Davidson potential [19] and taking advantage of supersymmetric quantum mechanics (SUSYQM) techniques [20, 21] developed in the study of quantum systems with mass depending on the coordinates [8, 9, 22].

It should be noticed that the Davidson potential [19], initially introduced for the description of molecular spectra, has been used for the description of nuclei since long ago [23, 24]. A major step forward has been the clarification of its group theoretical structure when used within the Bohr Hamiltonian, which was proved to be $SU(1,1) \times SO(5)$ [25]. This breakthrough led to the development of the algebraic collective model, a very rapidly converging approach allowing the calculation of spectra and transition probabilities of nuclei of any shape [26–29].

In the present work we consider the deformation dependent mass (DDM) Bohr Hamiltonian with a Kratzer potential [30]. This potential, also used initially in molecular physics, has been first used for the description of nuclei by Fortunato and Vitturi [31, 32]. We are motivated by the following questions.

(i) It is known that in the SUSYQM framework [9, 20, 21] the functional form of the dependence of the mass on the deformation is different for each potential. A first challenge is to prove that a DDM solution exists for the Bohr Hamiltonian with a Kratzer potential, and to find the form of this functional dependence.

(ii) The shapes of the Davidson [19] and Kratzer [30] potentials, shown in Fig. 1, are similar for small values of β , where the $1/\beta^2$ term dominates in both cases, but they differ substantially at large values of β , where the tails of the wave functions behave as $e^{-\beta^2/2}$ [33] and $e^{-\beta/2}$ [31, 32] respectively. It is interesting to examine to what extent numerical results for spectra and $B(E2)$ transition rates are influenced by the change in the potential. The level spacings within the β_1 band, which are usually overestimated by collective models based on the Bohr Hamiltonian, including the DDM Davidson model, are of

particular interest.

(iii) The DDM Bohr Hamiltonian with the Davidson potential works well for deformed nuclei, but fails in describing the nuclei lying at the critical point between the spherical and deformed regions [34, 35], known to be examples of the X(5) critical point symmetry [36]. It is interesting to examine if the DDM Bohr Hamiltonian with the Kratzer potential overcomes this drawback.

In Section II the DDM Bohr Hamiltonian is briefly reviewed, while in Section III the special case of the Kratzer potential is considered. Analytical expressions for spectra and wave functions are given in Sections IV and V respectively, while the calculation of $B(E2)$ transition rates is described in Section VI. Numerical results for spectra and $B(E2)$ transition rates are given in Section VII, while Section VIII contains the conclusions and plans for further work. The use of the deformed shape invariance principle for the construction of the spectrum is given in Appendix 1, while many technical details concerning the wave functions are given in Appendices 2-6. Finally, in Appendix 7, scaling factors are discussed.

II. BOHR HAMILTONIAN WITH DEFORMATION-DEPENDENT MASS

The original Bohr Hamiltonian [7] is

$$H_B = -\frac{\hbar^2}{2B} \left[\frac{1}{\beta^4} \frac{\partial}{\partial \beta} \beta^4 \frac{\partial}{\partial \beta} + \frac{1}{\beta^2 \sin 3\gamma} \frac{\partial}{\partial \gamma} \sin 3\gamma \frac{\partial}{\partial \gamma} - \frac{1}{4\beta^2} \sum_{k=1,2,3} \frac{Q_k^2}{\sin^2(\gamma - \frac{2}{3}\pi k)} \right] + V(\beta, \gamma), \quad (1)$$

where β and γ are the usual collective coordinates, while Q_k ($k = 1, 2, 3$) are the components of angular momentum in the intrinsic frame, and B is the mass parameter, which is usually considered constant.

Allowing the mass to depend on the deformation coordinate β (which measures departure from spherical shape),

$$B(\beta) = \frac{B_0}{(f(\beta))^2}, \quad (2)$$

where B_0 is a constant and f a function of β only, the Bohr equation becomes [17]

$$H\Psi = \left[-\frac{1}{2} \frac{\sqrt{f}}{\beta^4} \frac{\partial}{\partial \beta} \beta^4 f \frac{\partial}{\partial \beta} \sqrt{f} - \frac{f^2}{2\beta^2 \sin 3\gamma} \frac{\partial}{\partial \gamma} \sin 3\gamma \frac{\partial}{\partial \gamma} + \frac{f^2}{8\beta^2} \sum_{k=1,2,3} \frac{Q_k^2}{\sin^2(\gamma - \frac{2}{3}\pi k)} + v_{eff} \right] \Psi = \epsilon \Psi, \quad (3)$$

where reduced energies

$$\epsilon = B_0 E / \hbar^2 \quad (4)$$

and reduced potentials

$$v = B_0 V / \hbar^2 \quad (5)$$

have been used, and [17]

$$v_{eff} = v(\beta, \gamma) + \frac{1}{4}(1 - \delta - \lambda)f\nabla^2 f + \frac{1}{2} \left(\frac{1}{2} - \delta \right) \left(\frac{1}{2} - \lambda \right) (\nabla f)^2, \quad (6)$$

where δ and λ are free parameters, stemming from the following cause. If the mass is position dependent, then it does not commute with the momentum. Therefore there are many ways to generalize the usual form of the kinetic energy in order to obtain a Hermitian operator. It was actually in Ref. [5] where it was proved that the most general form of such a Hermitian Hamiltonian contains two free parameters (denoted by δ and λ in the present work). In Section VII it will be seen that these parameters play practically no role in the present work.

Exact separation of variables can be achieved in the usual three cases.

a) γ -unstable nuclei, in which the potential $v(\beta, \gamma)$ depends only on the variable β , i.e. $v(\beta) = u(\beta)$ [37, 38], and the wave functions are of the form

$$\Psi(\beta, \gamma, \theta_i) = \xi(\beta)\Phi(\gamma, \theta_i), \quad (7)$$

where θ_i ($i = 1, 2, 3$) are the Euler angles.

b) Axially symmetric prolate deformed nuclei with $\gamma \approx 0$, in which the potential is assumed to be of the form [33, 37, 39-41]

$$v(\beta, \gamma) = u(\beta) + \frac{f^2}{\beta^2} w(\gamma), \quad (8)$$

with

$$w(\gamma) = \frac{1}{2}(3c)^2 \gamma^2, \quad (9)$$

where c is a free parameter, while the wave functions read [36]

$$\Psi(\beta, \gamma, \theta_i) = \xi_L(\beta)\eta_K(\gamma)\mathcal{D}_{M,K}^L(\theta_i), \quad (10)$$

where $\mathcal{D}(\theta_i)$ denote Wigner functions of the Euler angles, L is the angular momentum quantum number, while M and K are the quantum numbers of the projections of angular momentum on the laboratory-fixed z -axis and the body-fixed z' -axis respectively.

c) Triaxial nuclei with $\gamma \approx \pi/6$, in which again the potential is assumed to be of the form of Eq. (8), but with

$$w(\gamma) = \frac{1}{4}c \left(\gamma - \frac{\pi}{6} \right)^2, \quad (11)$$

while the wave functions read [42]

$$\Psi(\beta, \gamma, \theta_i) = \xi_{L,\alpha}(\beta)\eta(\gamma)\mathcal{D}_{M,\alpha}^L(\theta_i), \quad (12)$$

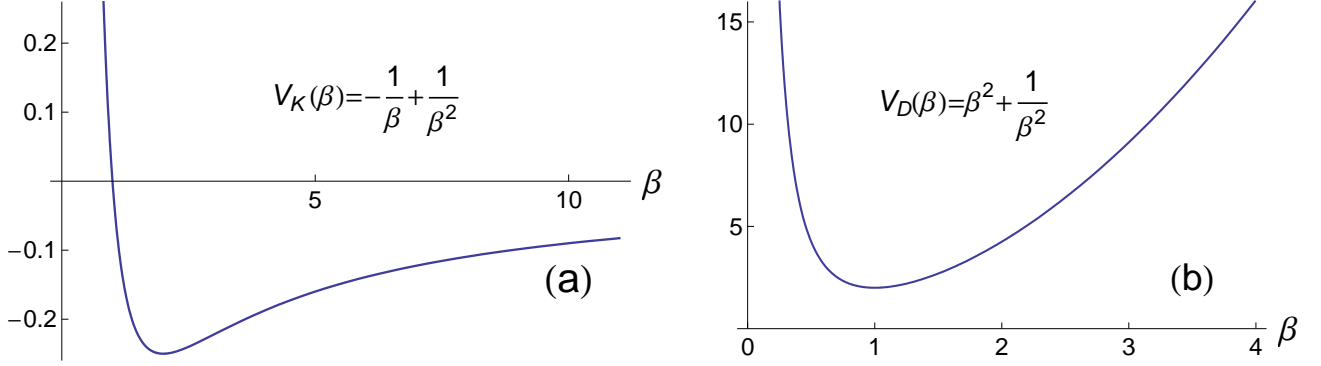


FIG. 1: (Color online) The Kratzer (left) and Davidson (right) potentials. The quantities shown are dimensionless, while all free parameters have been set equal to unity, for the sake of simplicity.

where $\mathcal{D}(\theta_i)$ denote Wigner functions of the Euler angles, L is the angular momentum quantum number, while M and α are the quantum numbers of the projections of angular momentum on the laboratory-fixed z -axis and the body-fixed x' -axis respectively.

The angular equations and wave functions can be found in Ref. [17]. The radial equations in all three cases take the common form [17]

$$HR(\beta) = -\left(\sqrt{f}\frac{d}{d\beta}\sqrt{f}\right)^2 R(\beta) + 2u_{eff}R(\beta) = 2\epsilon R(\beta), \quad (13)$$

where

$$\xi(\beta) = \frac{R(\beta)}{\beta^2}, \quad (14)$$

$$u_{eff} = u + \frac{1}{4}(1 - \delta - \lambda)f\left(\frac{4f'}{\beta} + f''\right) + \frac{1}{2}\left(\frac{1}{2} - \delta\right)\left(\frac{1}{2} - \lambda\right)(f')^2 + \frac{f^2 + \beta f f'}{\beta^2} + \frac{f^2}{2\beta^2}\Lambda, \quad (15)$$

f' (f'') denote the first (second) derivative of f , while Λ in each case acquires the following form.

a) For γ -unstable nuclei

$$\Lambda = \tau(\tau + 3), \quad (16)$$

with τ being the seniority quantum number [43]. The values of angular momentum L occurring for each τ are provided by a well known algorithm and are listed in [37, 44]. Within the ground state band (gsb) one has $L = 2\tau$.

b) For axially symmetric prolate deformed nuclei,

$$\Lambda = \frac{L(L+1) - K^2}{3} + (6c)(n_\gamma + 1), \quad (17)$$

where n_γ is the quantum number related to γ -oscillations.

c) For triaxial nuclei with $\gamma \approx \pi/6$,

$$\Lambda = \frac{L(L+4) + 3n_w(2L - n_w)}{4} + \sqrt{2c}\left(n_\gamma + \frac{1}{2}\right), \quad (18)$$

where $n_w = L - \alpha$ is the wobbling quantum number [45, 46].

III. THE KRATZER POTENTIAL

Up to now no assumption about the specific form of the potential $u(\beta)$ and the deformation function $f(\beta)$ has been made. From the results for 3-dimensional systems reported in Ref. [9], we know that for each potential a different deformation function is appropriate.

In Ref. [17], the Davidson potential [19]

$$u(\beta) = \beta^2 + \frac{\beta_0^4}{\beta^2}, \quad (19)$$

where the parameter β_0 indicates the position of the minimum of the potential, has been considered in the framework of the Bohr Hamiltonian, the appropriate deformation function being

$$f(\beta) = 1 + a\beta^2, \quad a \ll 1. \quad (20)$$

Here we are going to consider the Kratzer potential [30]

$$u(\beta) = -\frac{1}{\beta} + \frac{\tilde{B}}{\beta^2}, \quad (21)$$

for which the deformation function is expected [9] to be

$$f(\beta) = 1 + a\beta, \quad a \ll 1. \quad (22)$$

Using these forms for the potential and the deformation function in Eq. (15) one obtains

$$\begin{aligned} 2u_{\text{eff}} &= k_0 + \frac{k_{-1}}{\beta} + \frac{k_{-2}}{\beta^2}, \\ k_0 &= a^2[2(3 - \delta - \lambda) + \frac{1}{4}(1 - 2\delta)(1 - 2\lambda) + \Lambda], \\ k_{-1} &= -2 + 2a[(4 - \delta - \lambda) + \Lambda], \\ k_{-2} &= 2 + \Lambda + 2\tilde{B}, \end{aligned} \quad (23)$$

where a is the deforming parameter, δ and λ are free parameters coming from the construction procedure of the kinetic energy term [5] and going to be discussed further in Section VII.A, and Λ is the eigenvalue coming from the exact separation of variables, given by Eqs. (16), (17), (18), depending on the nature of the nucleus in discussion (γ -unstable, axially symmetric prolate deformed, triaxial with $\gamma \approx \pi/6$ respectively).

The radial equation for the Kratzer potential is solved in Appendix 1, using deformed shape invariance.

IV. ENERGY SPECTRUM

Using the results of Appendix 1, the energy spectrum of Eq. (13) is given by

$$\epsilon_n = \frac{1}{2} \left[k_0 - \left(\frac{k_{-1} + a \left[n^2 + \frac{1}{2}(1 + \Delta)(2n + 1) \right]}{2n + 1 + \Delta} \right)^2 \right], \quad n = 0, 1, 2, \dots, \quad (24)$$

where

$$\Delta \equiv \sqrt{1 + 4k_{-2}}. \quad (25)$$

Equation (24) only provides a formal solution to the bound-state energy spectrum. The range of n values is actually determined by the existence of corresponding physically acceptable wave functions, the relevant conditions being stated in Appendix 2.

In Eq. (24) the quantities k_0 , k_{-1} , k_{-2} are given by Eq. (23), in which Λ is given by Eq.(16), (17), or (18), for γ -unstable, axially symmetric prolate deformed, or triaxial nuclei respectively. The ground state band is obtained for $n = 0$, while for $n = 1$ and $n = 2$ the quasi- β_1 and quasi- β_2 bands are obtained respectively.

In the limit of no dependence of the mass on the deformation, i.e., $a \rightarrow 0$, one has from Eq. (23)

$$k_0 = 0, \quad k_{-1} = -2. \quad (26)$$

In this limit the spectrum becomes

$$\epsilon_n = -\frac{1}{2 \left(n + \frac{1}{2} + \frac{\Delta}{2} \right)^2}. \quad (27)$$

For γ -unstable nuclei this reads

$$\epsilon_n = -\frac{1}{2 \left(n + \frac{1}{2} + \sqrt{\left(\tau + \frac{3}{2} \right)^2 + 2\tilde{B}} \right)^2}, \quad (28)$$

in agreement with Eq. (11) of Ref. [31].

In the axially symmetric prolate deformed case the energies for the ground state and β bands in the limit $a \rightarrow 0$ read

$$\epsilon_n = -\frac{1}{2 \left(n + \frac{1}{2} + \sqrt{\frac{9}{4} + \frac{L(L+1)}{3}} + 2\tilde{B} \right)^2}, \quad (29)$$

in agreement with Eq. (10) of Ref. [32].

V. WAVE FUNCTIONS

The ground-state wavefunction is found in Appendix 3 to read

$$R_0(\beta) = N_0 \beta^{-\mu} f^{\frac{1}{2} \left(\mu + \frac{\tilde{K}}{\mu} - 1 \right)}, \quad (30)$$

where

$$\mu = -\frac{1}{2}(1 + \Delta), \quad (31)$$

while the normalization factor N_0 is given by Eq. (79), and \tilde{K} is given by Eq. (51).

As discussed in Appendix 3, this wave function is physically acceptable if the inequality

$$|\mu| = \frac{1}{2}(1 + \Delta) < -\frac{k_{-1}}{a}, \quad (32)$$

is satisfied by the parameters of the problem.

The excited state wave functions are found in Appendix 4 to be

$$\begin{aligned} R_n(\beta) &= N_n \beta^{-\mu_n} f^{\frac{1}{2} \left(\mu_n + \frac{\tilde{K}}{\mu_n} - 1 \right)} P_n^{\left(\mu_n - \frac{\tilde{K}}{\mu_n}, \mu_n + \frac{\tilde{K}}{\mu_n} \right)}(t), \\ t &= \frac{2 + a\beta}{a\beta}, \end{aligned} \quad (33)$$

where $\mu_n = \mu - n$, by $P_n^{(\alpha, \beta)}(t)$ the Jacobi polynomials [47] are denoted, while the normalization coefficient N_n is given by Eq. (80) in Appendix 5.

The reduction of the present wave functions to the form they have in the $a \rightarrow 0$ limit [31, 32] is carried out in Appendix 6.

VI. $B(E2)$ TRANSITION RATES

For the calculation of $B(E2)$ transition rates, the formulae given in Section X of Ref. [17] apply, with the wave functions $R_n(\beta)$ being replaced by the present results.

VII. NUMERICAL RESULTS

A. Spectra of γ -unstable nuclei

Rms fits of spectra have been performed, using the quality measure

$$\sigma = \sqrt{\frac{\sum_{i=1}^n (E_i(exp) - E_i(th))^2}{(n-1)E(2_1^+)^2}}. \quad (34)$$

The same set of experimental data for spectra and $B(E2)$ transition rates has been used as in the cases of the Deformation Dependent Mass (DDM) Davidson model [17], the Exactly Separable Davidson (ESD) model [33], and the Morse potential [48, 49], in order to facilitate comparisons of the various models among themselves and to the data.

The theoretical predictions for the levels are obtained from Eq. (24), the ground state band corresponding to $n = 0$ and the quasi- β_1 band having $n = 1$. The levels of the quasi- γ_1 band are obtained through their degeneracies to members of the ground state band, implied by the $SO(5) \supset SO(3)$ reduction rules [37, 44], also listed in Table I of Ref. [50]. Within the ground state band (gsb) one has $L = 2\tau$. The $L = 2$ member of the quasi- γ_1 band is degenerate with the $L = 4$ member of the gsb, the $L = 3, 4$ members of the quasi- γ_1 band are degenerate to the $L = 6$ member of the gsb, the $L = 5, 6$ members of the quasi- γ_1 band are degenerate to the $L = 8$ member of the gsb, and so on.

The results shown in Table I have been obtained for $\delta = \lambda = 0$. One can easily verify that different choices for δ and λ lead to a renormalization of the parameter values a and β_0 , the predicted energy levels remaining exactly the same.

Concerning the physical content of the parameter a , it is instructive to consider in detail in Table I the Xe isotopes, known [52] to lie in the γ -unstable region and already discussed in the framework of the DDM Davidson model [17]. They extend from the borders of the neutron shell (with $^{134}\text{Xe}_{80}$ lying just below the $N=82$ shell closure) to the midshell ($^{120}\text{Xe}_{66}$) and even beyond, exhibiting increasing collectivity (increasing $R_{4/2} = E(4_1^+)/E(2_1^+)$ ratios) from the border to the midshell.

Moving from the border of the neutron shell to the midshell, the following remarks apply.

- i) The Kratzer parameter \tilde{B} is increasing smoothly as one moves from the border towards the middle of the shell.
- ii) The a parameter, expressing the dependence of the mass on the deformation, is zero, or close to zero, for the first 4 isotopes close to the border, while it acquires substantially non-zero values for the last 5 isotopes close to mid-shell. This indicates that for nearly spherical nuclei no dependence of the mass on the deformation is needed, while it is becoming necessary as soon as substantial deviations from the spherical shape set in.

The effective potentials of Eq. (23) for some Xe isotopes, appropriately rescaled as described in Appendix 7, are shown in Fig. 2(a). It is clear that the potentials get deeper as one moves from the border of the neutron shell ($^{134}\text{Xe}_{80}$) to the midshell ($^{120}\text{Xe}_{66}$).

Other chains of isotopes also show similar behavior. As an example, the effective potentials of Eq. (23) for some Ba isotopes, appropriately rescaled as described in Appendix 7, are shown in Fig. 2(b). It is again clear that the potentials get deeper as one moves from the border of the neutron shell ($^{136}\text{Ba}_{80}$) towards the midshell ($^{122}\text{Ba}_{66}$).

The dependence of the effective potentials of Eq. (23) on the parameter a and on the angular momentum L is shown in Fig. 3, after appropriate rescaling according to Appendix 7. The effective potential of the $L = 4$ state of the ground state band of ^{130}Xe is used as the basis for the comparison. It is seen that the effective potential becomes less deep as the parameter a is increased. It also becomes less deep as the angular momentum L is increased.

It is remarkable that all effective potentials shown in Figs. 2 and 3 look qualitatively similar to the pure Kratzer potential of Fig. 1(left).

B. Spectra of axially symmetric deformed nuclei

Fits of spectra of deformed rare earth and actinide nuclei are shown in Table II. The energy levels are obtained from Eq. (24). The ground state band is obtained for $n = 0$ and the β_1 band for $n = 1$, while both have $n_\gamma = 0$ and $K = 0$. The γ_1 band is obtained for $n = 0$, $n_\gamma = 1$ and $K = 2$. Again, the choice $\delta = \lambda = 0$ has been made, and it is seen that different choices for δ and λ lead to a renormalization of the parameter values a , B , and c , the predicted energy levels remaining exactly the same.

The quality of the fits obtained can also be seen in Table III, where the calculated energy levels of ^{170}Er and ^{232}Th are compared to experiment.

The main discrepancy between theory and experiment in the case of the DDM Davidson [17] was found in the β_1 -bands, in which the theoretical level spacings were larger than the experimental ones. This was attributed to the shape of the Davidson potential, which raises to infinity at large β , pushing β bands higher and increasing their interlevel spacing. It is known that this problem can be avoided by using a potential going to some finite value at large β [53], like the Morse potential [54]. The Kratzer potential is going to zero for large β , thus avoiding the problem of the overestimation of the level spacings within the β_1 band, as seen clearly in Table III.

In Fig. 4 the effective potentials of Eq. (23) for some Gd and Dy isotopes, appropriately rescaled as described in Appendix 7, are shown. It is clear that the potentials get deeper as one moves from the border of the neutron shell towards the midshell.

Another difference between the DDM Davidson and the present DDM Kratzer model is that the former can-

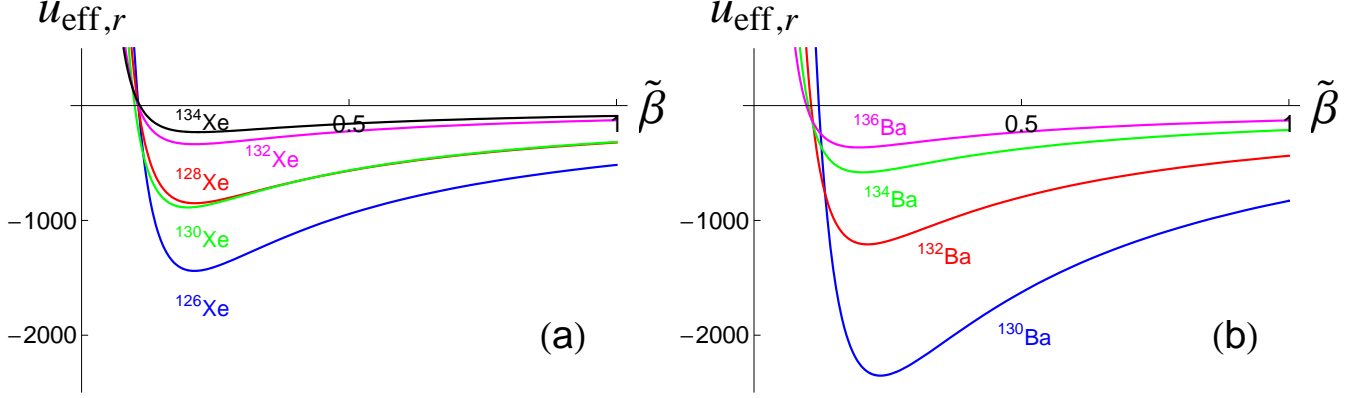


FIG. 2: (Color online) Effective potentials (Eq. (23)) for $L = 4$ for some Xe (a) and Ba (b) isotopes, corresponding to the parameters of Table I. The quantities shown are dimensionless. Rescaling has been carried out, according to Appendix 7, using the rescaling parameters A given in Table VII. The rescaled effective potentials are given by Eq. (127), while the rescaled abscissa, $\tilde{\beta}$, is given by Eq. (111).

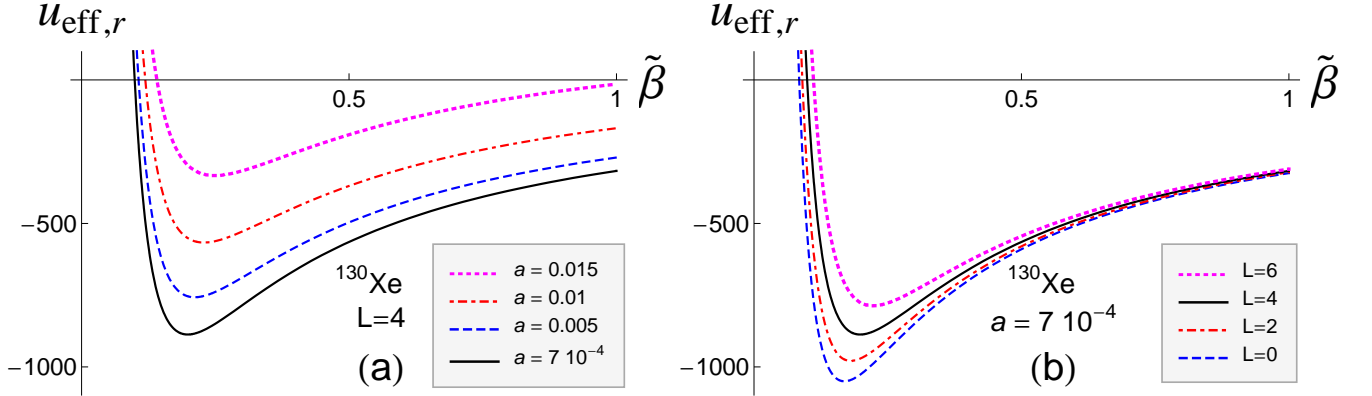


FIG. 3: (Color online) Dependence of the effective potentials of Eq. (23) on the parameter a [panel (a)] and on the angular momentum L [panel (b)]. The quantities shown are dimensionless. The effective potential for the $L = 4$ state of the ground state band of ^{130}Xe (corresponding to the parameters of Table I), plotted in both panels, is used as the basis of the comparison. Rescaling has been carried out, according to Appendix 7, using the rescaling parameters A given in Table VII. The rescaled effective potentials are given by Eq. (127), while the rescaled abscissa, $\tilde{\beta}$, is given by Eq. (111).

not describe the $N = 90$ isotones ^{150}Nd , ^{152}Sm , ^{154}Gd , and ^{156}Dy , which are considered [35] as the best examples of the X(5) [36] critical point symmetry, while in the latter a good description is obtained. Indeed, in Table II of Ref. [17] one sees that large σ deviations are obtained in the DDM Davidson case, while the spectra obtained in the present DDM Kratzer case are reported in Table IV, along with the parameter-free X(5) predictions [36, 55, 56]. In the β_1 bands, in particular, we see that the present approach, using the same number of parameters (three in the case of axially deformed nuclei) as the DDM Davidson model, avoids the overestimation of the interlevel spacings.

The ability of the DDM Kratzer model to describe the $N = 90$ isotones, in which the DDM Davidson model

fails, can be understood by considering the shapes of the two potentials. The Kratzer potential for appropriate parameter values can acquire the shape of a deep well, thus resembling the infinite square well potential used in the X(5) model [36], known to describe these $N = 90$ isotones.

In Fig. 5, the (rescaled according to Appendix 7) effective potentials for the $N = 90$ nuclei being good examples of the X(5) critical point symmetry are isolated, corroborating the remarks made above.

The dependence of the (rescaled according to Appendix 7) effective potentials of Eq. (23) on the parameter a and on the angular momentum L is shown in Fig. 6. The effective potential of the $L = 4$ state of the ground state band of ^{154}Gd is used as the basis for the compar-

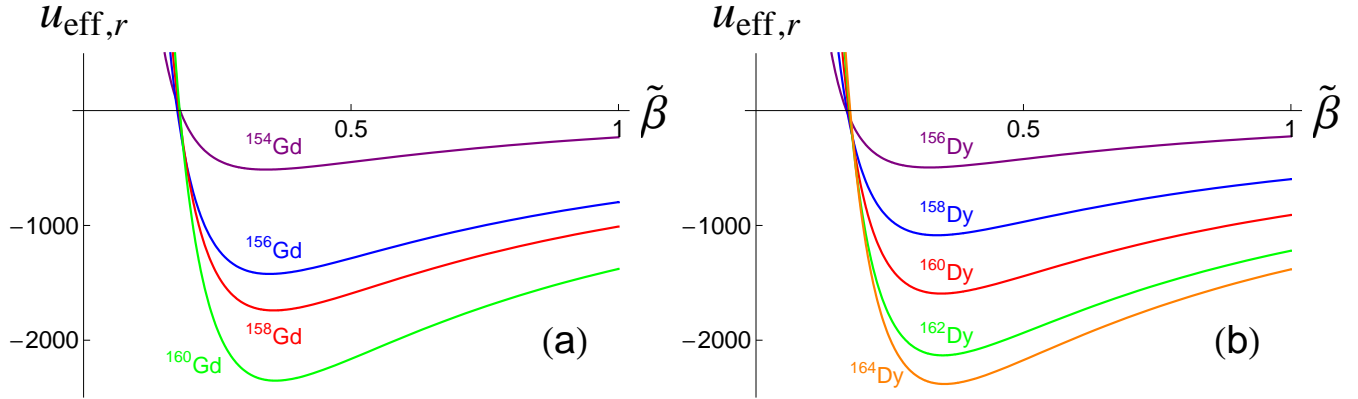


FIG. 4: (Color online) Effective potentials (Eq. (23)) for $L = 4$ for some Gd (a) and Dy (b) isotopes, corresponding to the parameters of Table II. The quantities shown are dimensionless. Rescaling has been carried out, according to Appendix 7, using the rescaling parameters A given in Table VIII. The rescaled effective potentials are given by Eq. (127), while the rescaled abscissa, $\tilde{\beta}$, is given by Eq. (111).

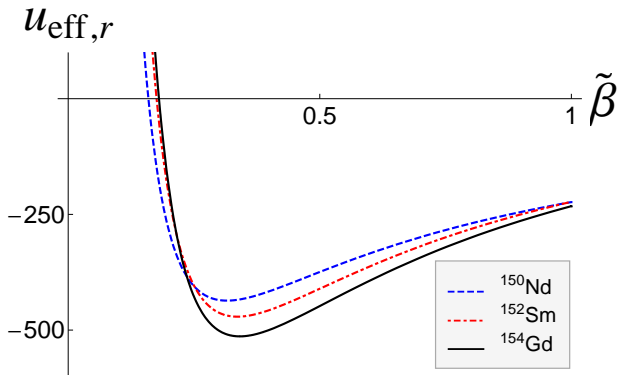


FIG. 5: (Color online) Effective potentials (Eq. (23)) for $L = 4$ for the $N = 90$ isotones being good examples of the X(5) critical point symmetry, corresponding to the parameters of Table II. The quantities shown are dimensionless. Rescaling has been carried out, according to Appendix 7, using the rescaling parameters A given in Table VIII. The rescaled effective potentials are given by Eq. (127), while the rescaled abscissa, $\tilde{\beta}$, is given by Eq. (111).

son. It is again seen that the effective potential becomes less deep as the parameter a is increased. It also becomes less deep as the angular momentum L is increased.

C. $B(E2)$ s of γ -unstable nuclei

$B(E2)$ s within the ground state band, as well as interband $B(E2)$ s for which experimental data exist for several nuclei, have been calculated using the procedure described in subsec. X.A of Ref. [17]. For each nucleus, the parameters obtained by fitting the spectra have been used. The results are shown in Table V, the overall agree-

ment being good.

D. $B(E2)$ s of axially symmetric deformed nuclei

$B(E2)$ s within the ground state band, as well as interband $B(E2)$ s for which experimental data exist for several nuclei, have been calculated using the procedure described in subsec. X.B of Ref. [17]. The results are shown in Table VI. In order to facilitate comparison with the $N = 90$ isotones ^{150}Nd , ^{152}Sm , ^{154}Gd , and ^{156}Dy , which are considered [35] as the best examples of the X(5) [36] critical point symmetry, the X(5) predictions [36, 55, 56] are shown in the first line of the table. The overall agreement is good, although interband transitions are usually overestimated by theory.

VIII. CONCLUSIONS

The main results of the present work are summarized here.

(i) Analytical solutions of the deformation dependent mass (DDM) Bohr Hamiltonian with the Kratzer potential have been obtained for γ -unstable, axially symmetric prolate deformed, and triaxial nuclei. The deformation function for the Kratzer potential was found to be $f(\beta) = 1 + a\beta$, to be compared with the deformation function $f(\beta) = 1 + a\beta^2$ obtained in the case of the Davidson potential [17].

(ii) Despite the fact that the Davidson and Kratzer potentials have very different shapes, numerical results coming from fitting the spectra of more than 100 nuclei and then using the same parameters for calculating $B(E2)$ transition rates, indicate that good overall agreement to the experimental data is achieved in both cases.

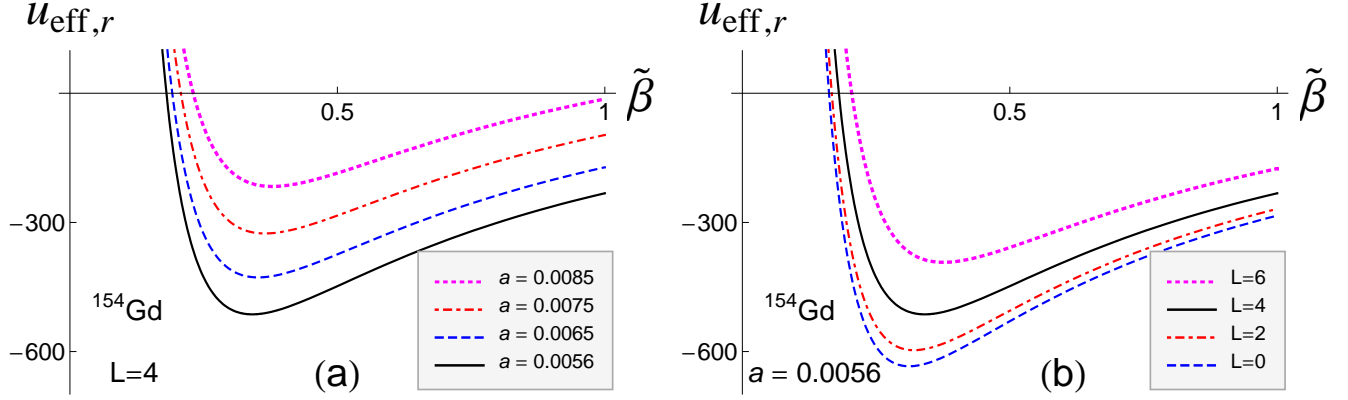


FIG. 6: (Color online) Dependence of the effective potentials of Eq. (23) on the parameter a [panel (a)] and on the angular momentum L [panel (b)]. The quantities shown are dimensionless. The effective potential for the $L = 4$ state of the ground state band of ^{154}Gd (corresponding to the parameters of Table II), plotted in both panels, is used as the basis of the comparison. Rescaling has been carried out, according to Appendix 7, using the rescaling parameters A given in Table VIII. The rescaled effective potentials are given by Eq. (127), while the rescaled abscissa, $\tilde{\beta}$, is given by Eq. (111).

Therefore the important factor in obtaining spectra with proper dependence of the moment of inertia on the deformation is the dependence of the mass on the deformation, independently of the particular shape of the potential.

(iii) On the other hand, a substantial difference between the two potentials shows up in the level spacings within the β_1 band. While these spacings are usually overestimated by collective models based on the Bohr Hamiltonian, the DDM Davidson model included, the present DDM Kratzer model avoids this problem, using the same number of parameters as the DDM Davidson model.

(iv) Furthermore, the Kratzer potential is able to acquire the shape of a deep narrow well, while the Davidson potential cannot achieve this. As a result, the DDM Bohr Hamiltonian with the Kratzer potential succeeds in describing the $N = 90$ rare earths which are considered as hallmark examples [34, 35] of the $X(5)$ critical point symmetry [36] between spherical and deformed nuclei.

The physical content of the free parameter a appearing in the dependence of the mass on the deformation can be further investigated in at least two ways:

(i) By exploiting the equivalence of the deformation dependence of the mass to a curved space [8].

(ii) By considering the similarity of several terms appearing in the DDM Bohr Hamiltonian to the Hamiltonian of the classical limit [57] of the interacting boson model [44].

Work in these directions is in progress.

Acknowledgements

The authors are thankful to F. Iachello for suggesting the project and for useful discussions. One of authors (N.

M.) acknowledges the support of the Bulgarian Scientific Fund under contract DID-02/16-17.12.2009.

Appendix 1: Deformed shape invariance

H may be considered as the first member $H_0 = H$ of a hierarchy of Hamiltonians

$$H_i = A_i^+ A_i^- + \sum_{j=0}^i \varepsilon_j, \quad i = 0, 1, 2, \dots, \quad (35)$$

where the first-order operators [9]

$$A_i^\pm = A^\pm(\mu_i, \nu_i) = \mp \sqrt{f} \frac{d}{d\beta} \sqrt{f} + W(\mu_i, \nu_i; \beta) \quad (36)$$

satisfy a deformed shape invariance condition

$$A_i^- A_i^+ = A_{i+1}^+ A_{i+1}^- + \varepsilon_{i+1}, \quad i = 0, 1, 2, \dots, \quad (37)$$

with ε_i , $i = 0, 1, 2, \dots$, denoting some constants. In other words, the superpotential $W(\mu, \nu; \beta)$ fulfils the two conditions

$$W^2(\mu, \nu; \beta) - f(\beta)W'(\mu, \nu; \beta) + \varepsilon_0 = 2u_{\text{eff}}(\beta), \quad (38)$$

and

$$\begin{aligned} W^2(\mu_i, \nu_i; \beta) + f(\beta)W'(\mu_i, \nu_i; \beta) = \\ W^2(\mu_{i+1}, \nu_{i+1}; \beta) - f(\beta)W'(\mu_{i+1}, \nu_{i+1}; \beta) + \varepsilon_{i+1}, \\ i = 0, 1, 2, \dots, \end{aligned} \quad (39)$$

where $\mu_0 = \mu$, $\nu_0 = \nu$, and a prime denotes derivative with respect to β .

In the case of the effective potential given in Eq. (23), $W(\mu, \nu; \beta)$ is a class 1 superpotential

$$W(\mu, \nu; \beta) = \mu\phi(\beta) + \nu, \quad (40)$$

$$\phi(\beta) = \frac{1}{\beta}, \quad (41)$$

which means that Eqs. (3.9) and (3.10) of [9] read

$$\begin{aligned} \phi'(\beta) &= -\frac{1}{\beta^2} = \frac{A}{\beta^2} + \frac{B}{\beta} + C, \\ a\beta &= \frac{(A'/\beta^2) + (B'/\beta) + C'}{(-1/\beta^2)}, \end{aligned} \quad (42)$$

with $A = -1$, $B = C = 0$, $A' = 0$, $B' = -a$ and $C' = 0$.

Inserting Eqs. (40) and (41) in (38), we obtain

$$\left(\frac{\mu}{\beta} + \nu\right)^2 - (1 + a\beta) \left(-\frac{\mu}{\beta^2}\right) + \varepsilon_0 = k_0 + \frac{k_{-1}}{\beta} + \frac{k_{-2}}{\beta^2}, \quad (43)$$

which is equivalent to the three equations

$$\mu(\mu + 1) = k_{-2}, \quad \mu(2\nu + a) = k_{-1}, \quad \nu^2 + \varepsilon_0 = k_0. \quad (44)$$

Their solutions read

$$\begin{aligned} \mu &= \frac{1}{2}(-1 \pm \Delta), \quad \nu = \frac{k_{-1} - a\mu}{2\mu}, \quad \varepsilon_0 = k_0 - \nu^2, \\ \Delta &\equiv \sqrt{1 + 4k_{-2}}, \end{aligned} \quad (45)$$

where we note that $1 + 4k_{-2}$ is always positive. As we shall show in Appendix 2, the conditions ensuring that the ground state wavefunction is physically acceptable select the lower sign for μ :

$$\mu = -\frac{1}{2}(1 + \Delta). \quad (46)$$

Inserting next Eqs. (40) and (41) in Eq. (39), we get

$$\begin{aligned} \left(\frac{\mu_i}{\beta} + \nu_i\right)^2 + (1 + a\beta) \left(-\frac{\mu_i}{\beta^2}\right) &= \\ \left(\frac{\mu_{i+1}}{\beta} + \nu_{i+1}\right)^2 - (1 + a\beta) \left(-\frac{\mu_{i+1}}{\beta^2}\right) + \varepsilon_{i+1}, \end{aligned} \quad (47)$$

leading to the three conditions

$$\begin{aligned} \mu_i(\mu_i - 1) &= \mu_{i+1}(\mu_{i+1} + 1), \\ \mu_i(2\nu_i - a) &= \mu_{i+1}(2\nu_{i+1} + a), \\ \nu_i^2 &= \nu_{i+1}^2 + \varepsilon_{i+1}. \end{aligned} \quad (48)$$

Their solutions are

$$\begin{aligned} \mu_{i+1} &= \mu_i - 1, \quad 2\mu_{i+1}\nu_{i+1} = 2\mu_i\nu_i - a(\mu_i + \mu_{i+1}), \\ \varepsilon_{i+1} &= \nu_i^2 - \nu_{i+1}^2. \end{aligned} \quad (49)$$

Note that there is an other solution for μ_{i+1} , namely $\mu_{i+1} = -\mu_i$, but the alternating signs would not be

compatible with physically acceptable excited state wave functions. Finally, the iteration of the first two relations in (49) leads to

$$\mu_i = \mu - i, \quad \nu_i = \frac{2\mu(\nu - ai) + ai^2}{2(\mu - i)}. \quad (50)$$

For future use, it is worth observing that ν_i can be rewritten in terms of μ_i as

$$\nu_i = \frac{a}{2} \left(\mu_i - \frac{\tilde{K}}{\mu_i} \right), \quad \tilde{K} \equiv k_{-2} - \frac{k_{-1}}{a}. \quad (51)$$

From (50), it indeed follows that

$$\nu_i = \frac{a}{2} \left(\mu_i - \frac{\mu(\mu - \frac{2\nu}{a})}{\mu_i} \right), \quad (52)$$

while Eq. (44) leads to

$$k_{-2} - \frac{k_{-1}}{a} = \mu \left(\mu - \frac{2\nu}{a} \right). \quad (53)$$

The energy spectrum of Eq. (13) is therefore given by

$$\begin{aligned} \epsilon_n &= \frac{1}{2} \sum_{i=0}^n \varepsilon_i = \frac{1}{2} (k_0 - \nu_n^2) \\ &= \frac{1}{2} \left[k_0 - \left(\frac{k_{-1} + a \left[n^2 + \frac{1}{2}(1 + \Delta)(2n + 1) \right]}{2n + 1 + \Delta} \right)^2 \right], \\ n &= 0, 1, 2, \dots \end{aligned} \quad (54)$$

Appendix 2: Conditions for physically acceptable wave functions

To be physically acceptable, the bound-state wavefunctions should satisfy two conditions [9]:

(i) As in conventional (constant-mass) quantum mechanics, they should be square integrable on the interval of definition of u_{eff} , i.e.,

$$\int_0^\infty d\beta |R_n(\beta)|^2 < \infty. \quad (55)$$

(ii) Furthermore, they should ensure the Hermiticity of H . For such a purpose, it is enough to impose that the operator $-i\sqrt{f}(d/d\beta)\sqrt{f}$ be Hermitian, which amounts to the restriction

$$|R_n(\beta)|^2 f(\beta) \rightarrow 0 \quad \text{for } \beta \rightarrow 0 \text{ and } \beta \rightarrow \infty, \quad (56)$$

or, equivalently,

$$\begin{aligned} |R_n(\beta)|^2 &\rightarrow 0 \quad \text{for } \beta \rightarrow 0 \quad \text{and} \\ |R_n(\beta)|^2 \beta &\rightarrow 0 \quad \text{for } \beta \rightarrow \infty. \end{aligned} \quad (57)$$

As condition (57) is more stringent than condition (55), we should only be concerned with the former.

Appendix 3: Ground-state wavefunction

The ground-state wavefunction, which is annihilated by A^- , is given by Eq. (2.29) of [9] as

$$R_0(\beta) = R_0(\mu, \nu; \beta) = \frac{N_0}{\sqrt{f(\beta)}} \exp \left(- \int^\beta \frac{W(\mu, \nu; \tilde{\beta})}{f(\tilde{\beta})} d\tilde{\beta} \right), \quad (58)$$

where N_0 is some normalization coefficient. Here

$$\begin{aligned} \int^\beta \frac{W(\mu, \nu; \tilde{\beta})}{f(\tilde{\beta})} d\tilde{\beta} &= \int^\beta \left(\frac{\mu}{\tilde{\beta}} + \frac{\nu - a\mu}{1 + a\tilde{\beta}} \right) d\tilde{\beta} \\ &= \mu \ln \beta + \frac{1}{a} (\nu - a\mu) \ln(1 + a\beta). \end{aligned} \quad (59)$$

Hence

$$R_0(\beta) = N_0 \beta^{-\mu} f^{-\frac{\nu - a\mu}{a} - \frac{1}{2}} = N_0 \beta^{-\mu} f^{\frac{1}{2}(\mu + \frac{\tilde{K}}{\mu} - 1)}, \quad (60)$$

where in the last step we used Eq. (51) for $i = 0$.

For $\beta \rightarrow 0$, the function $|R_0(\beta)|^2$ behaves as $\beta^{-2\mu}$. Condition (57) imposes that $\mu < 0$. Since k_{-2} , defined in Eq. (23), is greater than 2, it follows that Δ , defined in (45), is greater than 3, so that the upper sign choice for μ in (45) would lead to $\mu > 1$. As this is not acceptable, we have to take the lower sign for which $\mu < -2$.

For $\beta \rightarrow \infty$, $|R_0(\beta)|^2 \beta$ behaves as $\beta^{-\mu + \frac{\tilde{K}}{\mu}}$. Condition (57) therefore imposes that $\tilde{K}/\mu < \mu$ or

$$\mu^2 < \tilde{K}. \quad (61)$$

On taking (44), (46) and (51) into account, this restriction can be rewritten as

$$|\mu| = \frac{1}{2}(1 + \Delta) < -\frac{k_{-1}}{a}. \quad (62)$$

A physically acceptable ground-state wavefunction therefore exists only if the inequality (62) is satisfied by the parameters of the problem.

Appendix 4: Excited-state wavefunctions

According to Eqs. (2.30), (3.18) and (3.19) of [9], the excited-state wavefunctions are given by

$$R_n(\beta) = R_n(\mu, \nu; \beta) \propto R_0(\mu_n, \nu_n; \beta) P_n(\mu, \nu; y), \quad y = \frac{1}{\beta}, \quad (63)$$

where $P_n(\mu, \nu; y)$ is an n th-degree polynomial in y , satisfying the equation

$$\begin{aligned} P_{n+1}(\mu, \nu; y) &= y(y + a) \frac{d}{dy} P_n(\mu_1, \nu_1; y) \\ &+ [(\mu_{n+1} + \mu)y + \nu_{n+1} + \nu] P_n(\mu_1, \nu_1; y), \end{aligned} \quad (64)$$

with the starting value $P_0(\mu, \nu; y) = 1$.

From Eqs. (51) and (60), it follows that

$$\begin{aligned} R_n(\beta) &\propto \beta^{-\mu_n} f^{-\frac{\nu_n - a\mu_n}{a} - \frac{1}{2}} P_n(\mu, \nu; y) \\ &\propto \beta^{-\mu_n} f^{\frac{1}{2}(\mu_n + \frac{\tilde{K}}{\mu_n} - 1)} P_n(\mu, \nu; y). \end{aligned} \quad (65)$$

For $\beta \rightarrow 0$, the function $|R_n(\beta)|^2$ behaves as $\beta^{-2\mu_n - 2n} = \beta^{-2\mu}$, which goes to zero as it should be. For $\beta \rightarrow \infty$, $|R_n(\beta)|^2 \beta$ behaves as $\beta^{-\mu_n + \frac{\tilde{K}}{\mu_n}}$. Condition (57) therefore imposes that

$$\mu_n^2 < \tilde{K}, \quad (66)$$

which is equivalent to

$$n^2 + (2n + 1)|\mu| = n^2 + \left(n + \frac{1}{2}\right)(1 + \Delta) < -\frac{k_{-1}}{a}. \quad (67)$$

We conclude that there is a finite number of bound-state wavefunctions corresponding to $n = 0, 1, \dots, n_{\max}$, where n_{\max} is such that

$$\begin{aligned} n_{\max}^2 + \left(n_{\max} + \frac{1}{2}\right)(1 + \Delta) &< -\frac{k_{-1}}{a} \\ &\leq (n_{\max} + 1)^2 + \left(n_{\max} + \frac{3}{2}\right)(1 + \Delta). \end{aligned} \quad (68)$$

It now remains to solve Eq. (64). For such a purpose, let us make the changes of variable and of function

$$t = \frac{2y + a}{a}, \quad P_n \left(\mu, \frac{a}{2} \left(\mu - \frac{\tilde{K}}{\mu} \right); y \right) = C_n^{(\mu)} Q_n(\mu; t), \quad (69)$$

where $C_n^{(\mu)}$ is some constant. From definition (69), it follows that $Q_n(\mu; t)$ is an n th-degree polynomial in t . We successively get

$$y = \frac{a}{2}(t - 1), \quad y + a = \frac{a}{2}(t + 1), \quad \frac{d}{dy} = \frac{2}{a} \frac{d}{dt}. \quad (70)$$

By taking Eq. (51) into account, it is then straightforward to show that Eq. (64) becomes

$$\begin{aligned} \frac{2C_{n+1}^{(\mu)}}{aC_n^{(\mu-1)}} Q_{n+1}(\mu; t) &= \left\{ -(1 - t^2) \frac{d}{dt} + (2\mu_{n+1} + n + 1) \right. \\ &\times \left. \left(t - \frac{\tilde{K}}{\mu_{n+1}(\mu_{n+1} + n + 1)} \right) \right\} Q_n(\mu - 1; t). \end{aligned} \quad (71)$$

On taking into account that the Jacobi polynomials satisfy the equation

$$\begin{aligned} \frac{2(n + 1)(n + \alpha + \beta + 1)}{2n + \alpha + \beta + 2} P_{n+1}^{(\alpha, \beta)}(z) \\ = \left\{ -(1 - z^2) \frac{d}{dz} + (n + \alpha + \beta + 1) \right. \\ \times \left. \left(z + \frac{\alpha - \beta}{2n + \alpha + \beta + 2} \right) \right\} P_n^{(\alpha, \beta)}(z), \end{aligned} \quad (72)$$

obtained by combining their recurrence and differential relations (Eqs. (22.7.1) and (22.8.1) of [47]), we see that $Q_n(\mu - 1; t)$ is actually some Jacobi polynomial

$$Q_n(\mu - 1; t) = P_n^{\left(\mu_{n+1} - \frac{\tilde{K}}{\mu_{n+1}}, \mu_{n+1} + \frac{\tilde{K}}{\mu_{n+1}}\right)}(t), \quad (73)$$

provided we choose

$$\frac{C_{n+1}^{(\mu)}}{C_n^{(\mu-1)}} = \frac{a}{2} \frac{(n+1)(2\mu_{n+1} + n + 1)}{\mu_{n+1} + n + 1}, \quad C_0^{(\mu-n-1)} = 1, \quad (74)$$

or, in other words,

$$C_n^{(\mu)} = \left(\frac{a}{2}\right)^n \frac{n! \Gamma(2\mu - n + 1) \Gamma(\mu - n + 1)}{\Gamma(2\mu - 2n + 1) \Gamma(\mu + 1)}. \quad (75)$$

We therefore conclude that the wavefunctions are given by

$$R_n(\beta) = N_n \beta^{-\mu_n} f^{\frac{1}{2}}\left(\mu_n + \frac{\tilde{K}}{\mu_n} - 1\right) P_n^{\left(\mu_n - \frac{\tilde{K}}{\mu_n}, \mu_n + \frac{\tilde{K}}{\mu_n}\right)}(t), \quad t = \frac{2 + a\beta}{a\beta}, \quad (76)$$

where N_n is some normalization coefficient.

Appendix 5: Normalization coefficient

To calculate N_n , let us first express the whole wavefunction R_n in terms of t :

$$R_n = N_n \left(\frac{a}{2}\right)^{\mu_n} (t-1)^{\frac{1}{2}\left(\mu_n - \frac{\tilde{K}}{\mu_n} + 1\right)} (t+1)^{\frac{1}{2}\left(\mu_n + \frac{\tilde{K}}{\mu_n} - 1\right)} P_n^{\left(\mu_n - \frac{\tilde{K}}{\mu_n}, \mu_n + \frac{\tilde{K}}{\mu_n}\right)}(t). \quad (77)$$

From this we get

$$\int_0^\infty |R_n(\beta)|^2 d\beta = |N_n|^2 \left(\frac{a}{2}\right)^{2\mu_n-1} \int_1^\infty (t-1)^{\mu_n - \frac{\tilde{K}}{\mu_n} - 1} \times (t+1)^{\mu_n + \frac{\tilde{K}}{\mu_n} - 1} \left[P_n^{\left(\mu_n - \frac{\tilde{K}}{\mu_n}, \mu_n + \frac{\tilde{K}}{\mu_n}\right)}(t) \right]^2 dt. \quad (78)$$

For $n = 0$, the integral is easily calculated by using Eq. (3.196.2) of [58]. This leads to

$$N_0 = a^{-\mu+\frac{1}{2}} \left(\frac{\Gamma\left(-\mu - \frac{\tilde{K}}{\mu} + 1\right)}{\Gamma(-2\mu + 1) \Gamma\left(\mu - \frac{\tilde{K}}{\mu}\right)} \right)^{1/2}. \quad (79)$$

For $n \neq 0$, a similar integral follows from expanding the two Jacobi polynomials according to Eq. (22.3.1) of [47]

and integrating term by term. The result for N_n reads

$$N_n = a^{-\mu_n + \frac{1}{2}} \times \left[\Gamma\left(\mu_n - \frac{\tilde{K}}{\mu_n} + n + 1\right) \Gamma\left(\mu_n + \frac{\tilde{K}}{\mu_n} + n + 1\right) \right]^{-1} \times \left(\Gamma(-2\mu + 1) \sum_{m,p=0}^n \frac{A_n^{(m,p)}}{B_n^{(m,p)}} \right)^{-1/2}, \quad (80)$$

where

$$A_n^{(m,p)} = \Gamma\left(\mu_n - \frac{\tilde{K}}{\mu_n} + 2n - m - p\right), \quad B_n^{(m,p)} = m! (n-m)! p! (n-p)! \times \Gamma\left(\mu_n - \frac{\tilde{K}}{\mu_n} + n - m + 1\right) \Gamma\left(\mu_n + \frac{\tilde{K}}{\mu_n} + m + 1\right) \times \Gamma\left(\mu_n - \frac{\tilde{K}}{\mu_n} + n - p + 1\right) \Gamma\left(\mu_n + \frac{\tilde{K}}{\mu_n} + p + 1\right) \times \Gamma\left(-\mu_n - \frac{\tilde{K}}{\mu_n} - m - p + 1\right). \quad (81)$$

Appendix 6: Wave functions in the $a \rightarrow 0$ limit

In the present DDM Kratzer solution the wave functions contain Jacobi polynomials, while in the usual case [31, 32] they contain Laguerre polynomials. Contact between the two results should be established.

In the limit of no dependence of the mass on the deformation, i.e., $a \rightarrow 0$, one has

$$k_0 = 0, \quad k_{-1} = -2, \quad (82)$$

as well as

$$\tilde{K} = k_{-2} + \frac{2}{a}, \quad t = 1 + \frac{2}{a\beta}. \quad (83)$$

The last two quantities become infinite in the $a \rightarrow 0$ limit.

One should first notice that in the Jacobi polynomial of the present solution the variable β appears in the denominator, since $t = 1 + \frac{2}{a\beta}$, while in the Laguerre polynomials of the usual solution it appears in the numerator. Thus one should first use the identity (22.5.43 of [47])

$$P_n^{(\alpha,\beta)}(x) = \binom{2n + \alpha + \beta}{n} \left(\frac{x-1}{2}\right)^n {}_2F_1\left(-n, -n - \alpha; -2n - \alpha - \beta; \frac{2}{1-x}\right), \quad (84)$$

which in the present case leads to

$$P_n^{(\mu_n - \frac{\bar{K}}{\mu_n}, \mu_n + \frac{\bar{K}}{\mu_n})}(t) = \binom{2\mu}{n} \frac{1}{(a\beta)^n} {}_2F_1\left(-n, \frac{\bar{K}}{\mu - n} - \mu; -2\mu; -a\beta\right). \quad (85)$$

One should now implement the connection between hypergeometric functions and confluent hypergeometric functions. The hypergeometric functions ${}_2F_1(a, b; c; z)$ are solutions of the equation (p. 146 of Ref. [59])

$$z(1-z)\frac{d^2\phi}{dz^2} + [c - (a+b+1)z]\frac{d\phi}{dz} - ab\phi = 0. \quad (86)$$

Using the linear transformation $x = bz$ this leads to (page 148 of Ref. [59])

$$x\left(1 - \frac{x}{b}\right)\frac{d^2\phi}{dx^2} + \left[c - (a+1)\frac{x}{b} - x\right]\frac{d\phi}{dx} - a\phi = 0. \quad (87)$$

In the limit $b \rightarrow \infty$ this gives the equation

$$x\frac{d^2\phi}{dx^2} + (c-x)\frac{d\phi}{dx} - a\phi = 0, \quad (88)$$

which has as solutions the confluent hypergeometric functions ${}_1F_1(a; c; x)$. As a result, in the limit $b \rightarrow \infty$, the hypergeometric function ${}_2F_1(a, b; c; z)$ is reduced to the confluent hypergeometric function ${}_1F_1(a; c; x)$, where $x = bz$.

In the present case we consider the hypergeometric function

$${}_2F_1\left(-n, \frac{\bar{K}}{\mu - n} - \mu; -2\mu; -a\beta\right). \quad (89)$$

As mentioned above, in the limit $a \rightarrow 0$ the term \bar{K} becomes infinite. Thus the condition for the transition from ${}_2F_1(a, b; c; z)$ to ${}_1F_1(a; c; x)$ applies, leading to

$$\begin{aligned} & {}_1F_1\left(-n; -2\mu; -\left(\frac{\bar{K}}{\mu - n} - \mu\right)a\beta\right) \\ &= {}_1F_1\left(-n; \Delta + 1; -\left(\frac{\bar{K}}{\mu - n} - \mu\right)a\beta\right). \end{aligned} \quad (90)$$

One can now use the relation between confluent hypergeometric functions and Laguerre polynomials (p. 149 of Ref. [59])

$${}_1F_1(-n; m+1; z) = \frac{n!m!}{(n+m)!} L_n^{(m)}(z), \quad (91)$$

leading in the present case to

$$\begin{aligned} & {}_1F_1\left(-n; \Delta + 1; -\left(\frac{\bar{K}}{\mu - n} - \mu\right)a\beta\right) \\ &= \frac{n!\Delta!}{(n+\Delta)!} L_n^{(\Delta)}\left(-\left(\frac{\bar{K}}{\mu - n} - \mu\right)a\beta\right). \end{aligned} \quad (92)$$

From what we have seen above, n and $\mu = -\frac{1}{2}(1 + \Delta)$ remain finite, while $\bar{K} = k_{-2} + \frac{2}{a}$ becomes infinite because of the $1/a$ term, with k_{-2} remaining finite. Therefore in the argument of the Laguerre polynomial we can ignore the μ term as much smaller than the term containing \bar{K} , while within \bar{K} we can ignore the finite term k_{-2} in comparison to $1/a$, getting

$$\begin{aligned} & {}_1F_1\left(-n; \Delta + 1; \frac{2\beta}{\frac{1}{2}(1 + \Delta) + n}\right) \\ &= \frac{n!\Delta!}{(n+\Delta)!} L_n^{(\Delta)}\left(\frac{2\beta}{\frac{1}{2}(1 + \Delta) + n}\right). \end{aligned} \quad (93)$$

Concerning the factor $f^{\frac{1}{2}(\mu_n + \frac{\bar{K}}{\mu_n} - 1)}$ in Eq. (33), we remark that in the $a \rightarrow 0$ limit the term \bar{K} goes to infinity, while the other terms do not. From Eq. (83) it is clear that in this limit \bar{K} can be replaced by $2/a$. Thus one can write

$$F = f^{\frac{1}{2}(\mu_n + \frac{\bar{K}}{\mu_n} - 1)} \rightarrow f^{\frac{1}{a(\mu - n)}} = \left(\left(1 + \frac{\beta}{a^{-1}}\right)^{a^{-1}}\right)^{\frac{1}{\mu - n}}. \quad (94)$$

Taking advantage of Eq. (4.2.21) of Ref. [47]

$$\lim_{m \rightarrow \infty} \left(1 + \frac{z}{m}\right)^m = e^z, \quad (95)$$

the above factor becomes

$$F = (e^\beta)^{\frac{1}{\mu - n}} = \exp\left(-\frac{\beta}{n + \frac{1}{2} + \frac{\Delta}{2}}\right). \quad (96)$$

6.1 γ -unstable nuclei

The wave functions for γ -unstable nuclei are given in Ref. [31] (not normalized) and in Ref. [60] (normalized). Using the notation of Ref. [31] the normalized wave functions take the form

$$\chi(x)_{\tau, n} = \sqrt{\frac{n!}{\Gamma(n + 2\mu + 1)}} x^{\mu + \frac{1}{2}} e^{-x/2} L_n^{(2\mu)}(x), \quad (97)$$

where

$$\begin{aligned} x &= 2\beta\sqrt{\epsilon}, & \mu &= \sqrt{\left(\tau + \frac{3}{2}\right)^2 + D\beta_0^2}, \\ \sqrt{\epsilon} &= \frac{D\beta_0}{\mu + n + \frac{1}{2}}, \end{aligned} \quad (98)$$

and taking into account that in Ref. [31], the power of x appears as $2\mu + 1$ instead of $\mu + \frac{1}{2}$, because of a misprint.

In the DDM Kratzer case one has

$$\Lambda = \tau(\tau + 3) = \frac{L}{2} \left(\frac{L}{2} + 3\right) = \frac{1}{4}L(L + 6), \quad (99)$$

thus one gets

$$k_{-2} = 2 + \tau(\tau + 3) + 2\tilde{B},$$

$$\Delta = 2\sqrt{\left(\tau + \frac{3}{2}\right)^2 + 2\tilde{B}}, \quad (100)$$

leading in Eq. (97) the Laguerre polynomial into the form

$$L_n^{\left(2\sqrt{\left(\tau + \frac{3}{2}\right)^2 + 2\tilde{B}}\right)} \left(\frac{2\beta}{\sqrt{\left(\tau + \frac{3}{2}\right)^2 + 2\tilde{B} + \frac{1}{2} + n}} \right). \quad (101)$$

We see that with the parameter correspondence between the DDM Kratzer case and Ref. [31]

$$2\tilde{B} \rightarrow \beta_0, \quad 1 \rightarrow D\beta_0. \quad (102)$$

the Laguerre polynomials in the two expressions are identical. The exponential factor in Eq. (97) is also identical to the one of Eq. (96).

Written in the DDM parametrization the wave function of Ref. [31] reads

$$\chi^{(\beta)\tau,n} = \sqrt{\frac{n!}{\Gamma(n + 2\mu + 1)}} \left(\frac{2\beta}{\mu + \frac{1}{2} + n} \right)^{\mu + \frac{1}{2}}$$

$$\exp\left(\frac{-\beta}{\mu + \frac{1}{2} + n}\right) L_n^{(2\mu)}\left(\frac{2\beta}{\mu + \frac{1}{2} + n}\right), \quad (103)$$

where

$$\mu = \sqrt{\left(\tau + \frac{3}{2}\right)^2 + 2\tilde{B}}. \quad (104)$$

6.2 Axially symmetric prolate deformed nuclei

The wave functions for axially symmetric prolate deformed nuclei are given in Ref. [32] (not normalized) and in Ref. [60] (normalized). Using the notation of Ref. [32] the normalized wave functions take again the form of Eq. (97), but with

$$x = 2\beta\sqrt{\epsilon}, \quad \mu = \sqrt{\frac{L(L+1)}{3} + \frac{9}{4} + B},$$

$$\sqrt{\epsilon} = \frac{A/2}{\mu + n + \frac{1}{2}}. \quad (105)$$

In the DDM Kratzer case one has

$$\Lambda = \frac{L(L+1) - K^2}{3} + 6c(n_\gamma + 1), \quad c = \frac{C}{2}. \quad (106)$$

Since in Ref. [32] the approximate separation of variables introduced in X(5) is used, we formally put $c = 0$. For the

ground state band and the β -bands one also has $K = 0$. As a result we get

$$k_{-2} = 2 + \frac{L(L+1)}{3} + 2\tilde{B},$$

$$\Delta = 2\sqrt{\frac{9}{4} + \frac{L(L+1)}{3} + 2\tilde{B}}, \quad (107)$$

leading in Eq. (97) the Laguerre polynomial into the form

$$L_n^{\left(2\sqrt{\frac{9}{4} + \frac{L(L+1)}{3} + 2\tilde{B}}\right)} \left(\frac{2\beta}{\sqrt{\frac{9}{4} + \frac{L(L+1)}{3} + 2\tilde{B} + \frac{1}{2} + n}} \right). \quad (108)$$

We see that with the parameter correspondence between the DDM Kratzer case and Ref. [32]

$$2\tilde{B} \rightarrow B, \quad 2 \rightarrow A, \quad (109)$$

the Laguerre polynomials in the two expressions are identical. The exponential factor in Eq. (97) is also identical to the one of Eq. (96).

Written in the DDM parametrization the wave function of Ref. [32] reads again as Eq. (103), but with

$$\mu = \sqrt{\frac{L(L+1)}{3} + \frac{9}{4} + 2\tilde{B}}. \quad (110)$$

Appendix 7: Scaling factors

In the present work the Kratzer potential has been used in the form of Eq. (21), in which no free parameter appears in its first term. This choice does not affect ratios of energies and ratios of $B(E2)$ s, as it will be confirmed below. In this way the addition of an extra free parameter is avoided. If, however, one wishes to plot the effective potentials for different nuclei, this factor comes in and should be determined for each nucleus separately, as we shall see below.

7.1 Spectra

In the present work the Kratzer potential is used in the form of Eq. (21). In order to compare the results to the case in which a free parameter appears in the first term, we can use the rescaling transformation

$$\beta = \frac{\tilde{\beta}}{A}, \quad (111)$$

leading to

$$u(\tilde{\beta}) = -\frac{A}{\tilde{\beta}} + \frac{\tilde{B}_r}{\tilde{\beta}^2}, \quad \tilde{B}_r = A^2\tilde{B}. \quad (112)$$

In what follows we are going to use the subscript r for labelling rescaled quantities.

Using this rescaling in the original Bohr Hamiltonian of Eq. (1) we obtain

$$H_B = -\frac{\hbar^2}{2B_r} \left[\frac{1}{\tilde{\beta}^4} \frac{\partial}{\partial \tilde{\beta}} \tilde{\beta}^4 \frac{\partial}{\partial \tilde{\beta}} + \frac{1}{\tilde{\beta}^2 \sin 3\gamma} \frac{\partial}{\partial \gamma} \sin 3\gamma \frac{\partial}{\partial \gamma} - \frac{1}{4\tilde{\beta}^2} \sum_{k=1,2,3} \frac{Q_k^2}{\sin^2(\gamma - \frac{2}{3}\pi k)} \right] + V(\beta, \gamma), \quad (113)$$

with

$$B_r = \frac{B}{A^2}. \quad (114)$$

When allowing the nuclear mass to depend on the deformation as in Eq. (2), the rescaling leads to

$$B_r(\tilde{\beta}) = \frac{B_{0r}}{(f(\tilde{\beta}))^2}, \quad B_{0r} = \frac{B_0}{A^2}, \quad (115)$$

the deformation function of Eq. (22) becoming

$$f(\tilde{\beta}) = 1 + a_r \tilde{\beta}, \quad a_r = \frac{a}{A}. \quad (116)$$

From Eq. (114) it is clear that reduced energies, formerly defined through Eq. (4), now become

$$\epsilon_r = B_{0r} E / \hbar^2 = \frac{\epsilon}{A^2}. \quad (117)$$

This implies that

$$\epsilon = A^2 \epsilon_r, \quad (118)$$

in agreement to Eq. (11) of Ref. [31] and to Eq. (10) of Ref. [32], indicating that the energy levels scale as A^2 .

In the same way reduced potentials, formerly defined through Eq. (5), now become

$$v_r = B_{0r} V / \hbar^2 = \frac{v}{A^2}, \quad (119)$$

implying

$$v = A^2 v_r. \quad (120)$$

In axially symmetric prolate deformed nuclei, in which the potential is given in Eqs. (8) and (9), one gets

$$v(\tilde{\beta}, \gamma) = u(\tilde{\beta}) + \frac{f^2}{\tilde{\beta}^2} w_r(\gamma), \quad w_r(\gamma) = A^2 w(\gamma) \quad (121)$$

with

$$w_r(\gamma) = \frac{1}{2} (3c_r)^2 \gamma^2, \quad c_r = A c. \quad (122)$$

Similarly in triaxial nuclei with $\gamma \approx \pi/6$, in which the potential is assumed to be of the form of Eqs. (8) and (11), we obtain

$$w_r(\gamma) = \frac{1}{4} c_r \left(\gamma - \frac{\pi}{6} \right)^2, \quad c_r = A^2 c. \quad (123)$$

The effective potential of Eq. (15), in the Kratzer case, in which $f(\beta)$ is given by Eq. (22) and

$$f' = a, \quad f'' = 0, \quad (124)$$

takes the form

$$u_{eff} = -\frac{1}{\beta} + \frac{\tilde{B}}{\beta^2} + (1 - \delta - \lambda) f \frac{a}{\beta} + \frac{1}{2} \left(\frac{1}{2} - \delta \right) \left(\frac{1}{2} - \lambda \right) a^2 + \frac{f^2 + a\beta f}{\beta^2} + \frac{f^2}{2\beta^2} \Lambda, \quad (125)$$

with f given by Eq. (22). In rescaled notation the effective potential is written as

$$u_{eff} = -\frac{A}{\tilde{\beta}} + \frac{\tilde{B}_r}{\tilde{\beta}^2} + (1 - \delta - \lambda) f \frac{a_r}{\tilde{\beta}} A^2 + \frac{1}{2} \left(\frac{1}{2} - \delta \right) \left(\frac{1}{2} - \lambda \right) a_r^2 A^2 + \frac{f^2 + a_r \tilde{\beta} f}{\tilde{\beta}^2} A^2 + \frac{f^2}{2\tilde{\beta}^2} A^2 \Lambda, \quad (126)$$

with f given by Eq. (116). The rescaled effective potential, $u_{eff,r}(\tilde{\beta})$, is then calculated by plugging this result in the rhs of Eq. (119)

$$u_{eff,r} = \frac{u_{eff}}{A^2}. \quad (127)$$

7.2 Position of the minimum of the effective potential

It is instructive to study the position, β_0 , of the minimum of the effective potential, given in Eq. (23). Equating the derivative of the effective potential to zero we easily find for $\delta = \lambda = 0$

$$\beta_0 = -2 \frac{k_{-2}}{k_{-1}} = \frac{2 + \Lambda + 2\tilde{B}}{1 - 4a - a\Lambda}. \quad (128)$$

In the case of γ -unstable nuclei for the ground state ($\tau = 0$, $L = 0$) we obtain

$$\beta_0 = \frac{2 + 2\tilde{B}}{1 - 4a}. \quad (129)$$

Using Eq. (111) this leads to

$$A = \frac{1 - 4a}{2 + 2\tilde{B}} \tilde{\beta}_0. \quad (130)$$

In the case of prolate deformed nuclei for the ground state ($L = 0$, $n_\gamma = 0$) we obtain

$$\beta_0 = \frac{2 + 6c + 2\tilde{B}}{1 - 4a - 6ac}. \quad (131)$$

Using Eq. (111) this leads to

$$A = \frac{1 - 4a - 6ac}{2 + 6c + 2\tilde{B}} \tilde{\beta}_0. \quad (132)$$

7.3 Depth of the effective potential

As depth of the effective potential its value at the position of its minimum is considered. Substituting Eq. (128) in Eq. (23) we get

$$u_{\text{eff}}(\beta_0) = \frac{k_0}{2} - \frac{k_{-1}^2}{8k_{-2}}. \quad (133)$$

For $\delta = \lambda = 0$ this takes the form

$$u_{\text{eff}}(\beta_0) = \frac{a^2}{2} \left(\frac{25}{4} + \Lambda \right) - \frac{(1 - 4a - a\Lambda)^2}{4 + 2\Lambda + 4\tilde{B}}. \quad (134)$$

7.4 Comparison to the usual Kratzer potential

The usual Kratzer potential (without deformation dependence of the mass) in rescaled notation is given in Eq. (112). Equating the derivative of the effective potential to zero we easily find the position, $\tilde{\beta}_0$, of the minimum of the potential

$$\tilde{\beta}_0 = \frac{2\tilde{B}_r}{A}, \quad (135)$$

which in non-rescaled notation takes the form

$$\beta_0 = 2\tilde{B}, \quad (136)$$

where use of Eqs. (111) and (112) has been made.

We see that this expression is in agreement with Eq. (128) in the case of $a = 0$ and $\tilde{B} \gg 1$.

As mentioned above, as depth of the potential its value at the position of its minimum is considered. We then easily find

$$u(\tilde{\beta}_0) = -\frac{A^2}{4\tilde{B}_r}, \quad (137)$$

which in non-rescaled notation takes the form

$$u(\beta_0) = -\frac{1}{4\tilde{B}}, \quad (138)$$

where use of Eqs. (111) and (112) has been made.

We see that this expression is in agreement with Eq. (134) in the case of $a = 0$ and $\tilde{B} \gg 1$.

7.5 Wave functions

The wave functions $\xi(\beta)$ are normalized through

$$\int_0^\infty \beta^4 |\xi(\beta)|^2 d\beta = 1, \quad (139)$$

while the rescaled wave functions $\xi_r(\tilde{\beta})$ are normalized through

$$\int_0^\infty \tilde{\beta}^4 |\xi_r(\tilde{\beta})|^2 d\tilde{\beta} = 1. \quad (140)$$

From these relations one gets

$$\xi_r(\tilde{\beta}) = \frac{\xi(\beta)}{A^{5/2}}. \quad (141)$$

The wave functions $R(\beta)$ are normalized through

$$\int_0^\infty |R(\beta)|^2 d\beta = 1, \quad (142)$$

while the rescaled wave functions $R_r(\tilde{\beta})$ are normalized through

$$\int_0^\infty |R_r(\tilde{\beta})|^2 d\tilde{\beta} = 1. \quad (143)$$

From these relations one gets

$$R_r(\tilde{\beta}) = \frac{R(\beta)}{A^{1/2}}. \quad (144)$$

These results are consistent with Eq. (14), leading to

$$\xi_r(\tilde{\beta}) = \frac{R_r(\tilde{\beta})}{\tilde{\beta}^2}. \quad (145)$$

These results can also be checked against the explicit expressions for the wave functions.

In Eq. (30) we see that $R_0(\beta)$ will scale with $N_0\beta^{-\mu}$, while from Eq. (79) we see that N_0 will scale as $a^{-\mu+\frac{1}{2}}$. Therefore we get

$$R_0(\beta) \propto a^{-\mu+\frac{1}{2}}\beta^{-\mu} \quad (146)$$

and then in the rescaled framework

$$R_{0,r}(\tilde{\beta}) \propto a_r^{-\mu+\frac{1}{2}}\tilde{\beta}^{-\mu} = \left(\frac{a}{A}\right)^{-\mu+\frac{1}{2}}\tilde{\beta}^{-\mu} \propto A^{-1/2}R_0(\beta), \quad (147)$$

in agreement with Eq. (144).

Similarly, in Eq. (33) we see that $R_n(\beta)$ will scale with $N_n\beta^{-\mu_n}$, while from Eq. (80) we see that N_n will scale as $a^{-\mu_n+\frac{1}{2}}$. Therefore we get

$$R_n(\beta) \propto a^{-\mu_n+\frac{1}{2}}\beta^{-\mu_n} \quad (148)$$

and then in the rescaled framework

$$R_{n,r}(\tilde{\beta}) \propto a_r^{-\mu_n+\frac{1}{2}}\tilde{\beta}^{-\mu_n} = \left(\frac{a}{A}\right)^{-\mu_n+\frac{1}{2}}(A\beta)^{-\mu_n} \propto A^{-1/2}R_n(\beta), \quad (149)$$

in agreement with Eq. (144).

7.6 $B(E2)$ s

$B(E2)$ s are given by Eq. (B4) of Ref. [33], in which the square of the radial integral appears. The radial integral for γ -unstable nuclei is given in Eq. (116) of [17]

$$\begin{aligned} I_{n',\tau+1;n,\tau} &= \int_0^\infty \beta \xi_{n',\tau+1}(\beta) \xi_{n,\tau}(\beta) \beta^4 d\beta \\ &= \int_0^\infty \beta R_{n',\tau+1}(\beta) R_{n,\tau}(\beta) d\beta. \end{aligned} \quad (150)$$

From Appendix 7.5 it is clear that I behaves in scaling as β . In other words, in the rescaled framework we are going to have

$$I_r = AI. \quad (151)$$

Therefore in the rescaled framework for the $B(E2)$ s we are going to have

$$B(E2)_r = A^2 B(E2). \quad (152)$$

For prolate deformed nuclei, the radial integral is given by Eq. (117) of Ref. [17]. The same scaling properties occur then.

7.7 Numerical results

The numerical results on the spectra, reported in Tables I-IV, are not affected by rescaling since, according to Eq. (118), energies scale as A^2 , which cancels out when energy ratios are calculated.

Furthermore the numerical results on the $B(E2)$ s, reported in Tables V and VI, are not affected by rescaling, since the powers of A appearing because of the rescaling of wave functions, as described in Appendix 7.5, cancel out when $B(E2)$ ratios are calculated, as it is clear from Appendix 7.6.

The only results affected by scaling are the figures of the effective potential. From Eqs. (125) and (126) it is clear that the numerical values of the effective potentials are the same, irrespectively from calculating them in the rescaled framework or in the non-rescaled framework. Then the only rescaling entering is by an overall factor of A^2 , as seen in Eq. (120).

What is affected, however, is the abscissa. If the non-rescaled quantity β is used, it obtains very high numerical values, outside the region of physical interest. Here the rescaling procedure comes in. One way to obtain the value of the rescaling factor A for each nucleus is

to use it in order to have the minimum of the effective potential at the value of β corresponding to the quadrupole deformation of the specific nucleus obtained from $B(E2; 0_1^+ \rightarrow 2_1^+)$, i.e. from the transition rate from the ground state to the first excited state [61]. This can be done using Eq. (130) for γ -unstable nuclei, or Eq. (132) for prolate deformed nuclei.

Numerical values of the rescaling parameter A for the γ -unstable nuclei shown in Figs. 2 and 3 are shown in Table VII, while numerical values of A for the prolate deformed nuclei shown in Figs. 4, 5 and 6 are shown in Table VIII. Figs 2-6 have been drawn using these values of A . The potential values have been divided by A^2 , as indicated by Eq. (120), while in the abscissa β has been multiplied by A , according to Eq. (111).

As an extra qualitative check, the depth of each potential, which should have been approximately equal to $-1/(4\tilde{B})$ in a non-rescaled version of the figures 2-6, as discussed in Appendices 7.3 and 7.4, should be $-A^2/(4\tilde{B})$ in the rescaled version. For better accuracy, Eq. (134) should be used.

It should be noticed that the scale appropriate for each individual nucleus can be fixed in several ways.

1) Since energy levels scale as A^2 , as seen in Eq. (118), one way to determine A is by fitting it to the energy of the first excited state, $E(2_1^+)$, which is readily available for many nuclei [62].

2) Since $B(E2)$ s also scale as A^2 , as seen in Eq. (152), another way to determine A is by fitting it to the transition rate from the ground state to the first excited state, $B(E2; 0_1^+ \rightarrow 2_1^+)$, which is also readily available for many nuclei [61].

The method used here, namely fitting the minimum of the effective potential to the quadrupole deformation found from $B(E2; 0_1^+ \rightarrow 2_1^+)$, has the advantage that it avoids units, since β is a dimensionless quantity. It also avoids the scale factor appearing in the expression for the transition operator (see Eq. (115) of Ref. [17]).

-
- [1] D. J. BenDaniel and C. B. Duke, Phys. Rev. **152**, 683 (1966).
 - [2] T. Gora and F. Williams, Phys. Rev. **177**, 1179 (1969).
 - [3] G. Bastard, Phys. Rev. B **24**, 5693 (1981).
 - [4] Q.-G. Zhu and H. Kroemer, Phys. Rev. B **27**, 3519 (1983).
 - [5] O. von Roos, Phys. Rev. B **27**, 7547 (1983).
 - [6] R. A. Morrow, Phys. Rev. B **35**, 8074 (1987).
 - [7] A. Bohr, Mat. Fys. Medd. K. Dan. Vidensk. Selsk. **26**, no. 14 (1952).
 - [8] C. Quesne and V. M. Tkachuk, J. Phys. A: Math. Gen. **37**, 4267 (2004).
 - [9] B. Bagchi, A. Banerjee, C. Quesne, and V. M. Tkachuk, J. Phys. A: Math. Gen. **38**, 2929 (2005).
 - [10] R. V. Jolos and P. von Brentano, Phys. Rev. C **76**, 024309 (2007).
 - [11] R. V. Jolos and P. von Brentano, Phys. Rev. C **77**, 064317 (2008).
 - [12] R. V. Jolos and P. von Brentano, Phys. Rev. C **78**, 064309 (2008).
 - [13] R. V. Jolos and P. von Brentano, Phys. Rev. C **79**, 044310 (2009).
 - [14] R. V. Jolos and P. von Brentano, Phys. Rev. C **80**, 034308 (2009).
 - [15] M. J. Ermamatov and P. R. Fraser, Phys. Rev. C **84**, 044321 (2011).
 - [16] M. J. Ermamatov, P. C. Srivastava, P. R. Fraser, P. Stránský, and I. O. Morales, Phys. Rev. C **85**, 034307 (2012).
 - [17] D. Bonatsos, P. E. Georgoudis, D. Lenis, N. Minkov, and C. Quesne, Phys. Rev. C **83**, 044321 (2011).
 - [18] P. Ring and P. Schuck, *The Nuclear Many-Body Problem*

- (Springer, Berlin, 1980).
- [19] P. M. Davidson, Proc. R. Soc. London Ser. A **135**, 459 (1932).
 - [20] F. Cooper, A. Khare, and U. Sukhatme, Phys. Rep. **251**, 267 (1995).
 - [21] F. Cooper, A. Khare, and U. Sukhatme, *Supersymmetry in Quantum Mechanics* (World Scientific, Singapore, 2001).
 - [22] C. Quesne, J. Phys. A: Math. Theor. **40**, 13107 (2007).
 - [23] S. G. Rohoziński, J. Srebrny, and K. Horbaczewska, Z. Phys. **268**, 401 (1974).
 - [24] J. P. Elliott, J. A. Evans, and P. Park, Phys. Lett. B **169**, 309 (1986).
 - [25] D. J. Rowe and C. Bahri, J. Phys. A: Math. Gen. **31**, 4947 (1998).
 - [26] D. J. Rowe, Nucl. Phys. A **735**, 372 (2004).
 - [27] D. J. Rowe and P. S. Turner, Nucl. Phys. A **753**, 94 (2005).
 - [28] M. A. Caprio, Phys. Lett. B **672**, 396 (2009).
 - [29] D. J. Rowe, T. A. Welsh, and M. A. Caprio, Phys. Rev. C **79**, 054304 (2009).
 - [30] A. Kratzer, Z. Phys. **3**, 289 (1920).
 - [31] L. Fortunato and A. Vitturi, J. Phys. G: Nucl. Part. Phys. **29**, 1341 (2003).
 - [32] L. Fortunato and A. Vitturi, J. Phys. G: Nucl. Part. Phys. **30**, 627 (2004).
 - [33] D. Bonatsos, E. A. McCutchan, N. Minkov, R. F. Casten, P. Yotov, D. Lenis, D. Petrellis, I. Yigitoglu, Phys. Rev. C **76**, 064312 (2007).
 - [34] R. F. Casten and E. A. McCutchan, J. Phys. G: Nucl. Part. Phys. **34**, R285 (2007).
 - [35] P. Cejnar, J. Jolie, and R. F. Casten, Rev. Mod. Phys. **82**, 2155 (2010).
 - [36] F. Iachello, Phys. Rev. Lett. **87**, 052502 (2001).
 - [37] L. Wilets and M. Jean, Phys. Rev. **102**, 788 (1956).
 - [38] F. Iachello, Phys. Rev. Lett. **85**, 3580 (2000).
 - [39] L. Fortunato, Phys. Rev. C **70**, 011302 (2004).
 - [40] L. Fortunato, Eur. Phys. J. A **26** (s01), 1 (2005).
 - [41] L. Fortunato, S. De Baerdemacker, and K. Heyde, Phys. Rev. C **74**, 014310 (2006).
 - [42] D. Bonatsos, D. Lenis, D. Petrellis, and P. A. Terziev, Phys. Lett. B **588**, 172 (2004).
 - [43] D. R. Bès, Nucl. Phys. **10**, 373 (1959).
 - [44] F. Iachello and A. Arima, *The Interacting Boson Model* (Cambridge University Press, Cambridge, 1987).
 - [45] A. Bohr and B. R. Mottelson, *Nuclear Structure Vol. II: Nuclear Deformations* (Benjamin, New York, 1975).
 - [46] J. Meyer-ter-Vehn, Nucl. Phys. A **249**, 111 (1975).
 - [47] M. Abramowitz and I. A. Stegun, *Handbook of Mathematical Functions* (Dover, New York, 1965).
 - [48] I. Boztosun, D. Bonatsos, I. Inci, Phys. Rev. C **77**, 044302 (2008).
 - [49] I. Inci, D. Bonatsos, I. Boztosun, Phys. Rev. C **84**, 024309 (2011).
 - [50] D. Bonatsos, D. Lenis, N. Minkov, P. P. Raychev, and P. A. Terziev, Phys. Rev. C **69**, 044316 (2004).
 - [51] Nuclear Data Sheets, as of December 2005.
 - [52] R. F. Casten, *Nuclear Structure from a Simple Perspective* (Oxford University Press, Oxford, 1990).
 - [53] M. A. Caprio, Phys. Rev. C **65**, 031304(R) (2002).
 - [54] P. M. Morse, Phys. Rev. **34**, 57 (1929).
 - [55] D. Bonatsos, D. Lenis, N. Minkov, P. P. Raychev, and P. A. Terziev, Phys. Rev. C **69**, 014302 (2004).
 - [56] R. Bijker, R. F. Casten, N. V. Zamfir, and E. A. McCutchan, Phys. Rev. C **68**, 064304 (2003).
 - [57] J. N. Ginocchio and M. W. Kirson, Nucl. Phys. A **350**, 31 (1980).
 - [58] I. S. Gradshteyn and I. M. Ryzhik, *Table of Integral, Series, and Products* (Academic, New York, 1980).
 - [59] W. Greiner, *Quantum Mechanics* (Springer, Berlin, 1989).
 - [60] M. Moshinsky, T. H. Seligman, and K. B. Wolf, J. Math. Phys. **13**, 901 (1972).
 - [61] S. Raman, C. W. Nestor, Jr., and P. Tikkanen, At. Data Nucl. Data Tables **78**, 1 (2001).
 - [62] Brookhaven National Laboratory, National Nuclear Data Center, <http://www.nndc.bnl.gov/ensdf/>

TABLE I: Comparison of theoretical predictions of the γ -unstable Bohr Hamiltonian with β -dependent mass (with $\delta = \lambda = 0$) for the Kratzer potential to experimental data [51] of rare earth and actinides with $R_{4/2} \leq 2.6$ and known 0_2^+ and 2_1^+ states. The $R_{4/2} = E(4_1^+)/E(2_1^+)$ ratios, as well as the β and γ bandheads, normalized to the 2_1^+ state and labelled by $R_{0/2} = E(0_2^+)/E(2_1^+)$ and $R_{2/2} = E(2_1^+)/E(2_1^+)$ respectively, are shown. The angular momenta of the highest levels of the ground state, β and γ bands included in the rms fit are labelled by L_g , L_β , and L_γ respectively, while n indicates the total number of levels involved in the fit and σ is the quality measure of Eq. (34). The theoretical predictions are obtained from the formulae mentioned in Sec. IV. See subsec. VII A for further discussion.

nucleus	$R_{4/2}$ exp	$R_{4/2}$ th	$R_{0/2}$ exp	$R_{0/2}$ th	$R_{2/2}$ exp	$R_{2/2}$ th	\tilde{B}	a	L_g	L_β	L_γ	n	σ
⁹⁸ Ru	2.14	2.34	2.0	2.0	2.2	2.3	38	0.0101	24	0	4	15	0.811
¹⁰⁰ Ru	2.27	2.40	2.1	2.1	2.5	2.4	64	0.0094	24	0	4	15	0.824
¹⁰² Ru	2.33	2.35	2.0	2.0	2.3	2.3	41	0.0105	16	0	5	12	0.384
¹⁰⁴ Ru	2.48	2.39	2.8	3.1	2.5	2.4	60	0.0046	8	2	8	12	0.437
¹⁰² Pd	2.29	2.42	2.9	2.4	2.8	2.4	81	0.0072	24	4	4	17	0.996
¹⁰⁴ Pd	2.38	2.35	2.4	2.4	2.4	2.3	41	0.0072	18	2	4	13	0.328
¹⁰⁶ Pd	2.40	2.33	2.2	2.3	2.2	2.3	36	0.0082	16	4	5	14	0.398
¹⁰⁸ Pd	2.42	2.38	2.4	2.5	2.1	2.4	55	0.0069	14	4	4	12	0.317
¹¹⁰ Pd	2.46	2.43	2.5	2.7	2.2	2.4	100	0.0061	12	10	4	14	0.377
¹¹² Pd	2.53	2.32	2.6	2.6	2.1	2.3	33	0.0058	6	0	3	5	0.485
¹¹⁴ Pd	2.56	2.40	2.6	2.6	2.1	2.4	65	0.0065	16	0	11	18	0.772
¹¹⁶ Pd	2.58	2.42	3.3	3.3	2.2	2.4	83	0.0044	16	0	9	16	0.630
¹⁰⁶ Cd	2.36	2.33	2.8	2.8	2.7	2.3	36	0.0044	12	0	2	7	0.174
¹⁰⁸ Cd	2.38	2.34	2.7	2.7	2.5	2.3	39	0.0054	22	0	5	15	0.908
¹¹⁰ Cd	2.35	2.29	2.2	1.9	2.2	2.3	28	0.0115	16	6	5	15	0.341
¹¹² Cd	2.29	2.23	2.0	1.7	2.1	2.2	20	0.0126	12	8	11	20	0.282
¹¹⁴ Cd	2.30	2.25	2.0	1.7	2.2	2.2	22	0.0127	14	4	3	11	0.249
¹¹⁶ Cd	2.38	2.27	2.5	2.8	2.4	2.3	25	0.0028	14	2	3	10	0.306
¹¹⁸ Cd	2.39	2.29	2.6	2.6	2.6	2.3	28	0.0045	14	0	3	9	0.312
¹²⁰ Cd	2.38	2.31	2.7	2.7	2.6	2.3	32	0.0045	16	0	2	9	0.426
¹¹⁸ Xe	2.40	2.41	2.5	2.8	2.8	2.4	77	0.0058	16	4	10	19	0.408
¹²⁰ Xe	2.47	2.45	2.8	3.0	2.7	2.4	133	0.0049	26	4	9	23	0.701
¹²² Xe	2.50	2.45	3.5	3.5	2.5	2.4	131	0.0040	16	0	9	16	0.731
¹²⁴ Xe	2.48	2.43	3.6	3.7	2.4	2.4	93	0.0035	20	2	11	21	0.722
¹²⁶ Xe	2.42	2.39	3.4	3.4	2.3	2.4	60	0.0035	12	4	9	16	0.601
¹²⁸ Xe	2.33	2.31	3.6	3.7	2.2	2.3	32	0.0000	10	2	7	12	0.451
¹³⁰ Xe	2.25	2.30	3.3	3.3	2.1	2.3	29	0.0007	14	0	5	11	0.477
¹³² Xe	2.16	2.03	2.8	2.0	1.9	2.0	9	0.0000	6	0	5	7	0.374
¹³⁴ Xe	2.04	1.87	1.9	1.6	1.9	1.9	5	0.0000	6	0	5	7	0.216
¹³⁰ Ba	2.52	2.45	3.3	3.3	2.5	2.4	140	0.0043	12	0	6	11	0.392
¹³² Ba	2.43	2.37	3.2	3.2	2.2	2.4	50	0.0037	14	0	8	14	0.763
¹³⁴ Ba	2.32	2.20	2.9	2.8	1.9	2.2	18	0.0000	8	0	4	7	0.344
¹³⁶ Ba	2.28	2.00	1.9	1.9	1.9	2.0	8	0.0002	6	0	2	4	0.192
¹⁴² Ba	2.32	2.41	4.3	4.3	4.0	2.4	79	0.0021	14	0	2	8	0.591
¹³⁴ Ce	2.56	2.42	3.7	3.9	2.4	2.4	88	0.0030	28	2	8	22	0.882
¹³⁶ Ce	2.38	2.28	1.9	1.9	2.0	2.3	27	0.0105	16	0	3	10	0.546
¹³⁸ Ce	2.32	2.13	1.9	1.9	1.9	2.1	13	0.0083	14	0	2	8	0.350
¹⁴⁰ Nd	2.33	2.09	1.8	1.8	1.9	2.1	11	0.0073	6	0	2	4	0.168
¹⁴⁸ Nd	2.49	2.42	3.0	3.3	4.1	2.4	90	0.0042	12	8	4	13	0.719
¹⁴⁰ Sm	2.35	2.36	1.9	1.9	2.7	2.4	44	0.0115	8	0	2	5	0.161
¹⁴² Sm	2.33	2.16	1.9	1.9	2.2	2.2	15	0.0089	8	0	2	5	0.114
¹⁴² Gd	2.35	2.33	2.7	2.6	1.9	2.3	35	0.0054	16	0	2	9	0.290
¹⁴⁴ Gd	2.35	2.35	2.5	2.5	2.5	2.3	41	0.0065	6	0	2	4	0.108
¹⁵² Gd	2.19	2.34	1.8	1.9	3.2	2.3	40	0.0116	16	10	7	19	0.382
¹⁵⁴ Dy	2.23	2.40	2.0	1.7	3.1	2.4	67	0.0124	26	10	7	24	0.948
¹⁵⁶ Er	2.32	2.38	2.7	2.7	2.7	2.4	56	0.0062	20	4	5	16	0.357

TABLE I: (continued)

nucleus	$R_{4/2}$ exp	$R_{4/2}$ th	$R_{0/2}$ exp	$R_{0/2}$ th	$R_{2/2}$ exp	$R_{2/2}$ th	\tilde{B}	a	L_g	L_β	L_γ	n	σ
^{186}Pt	2.56	2.47	2.5	3.6	3.2	2.5	249	0.0035	26	6	10	25	0.791
^{188}Pt	2.53	2.43	3.0	3.2	2.3	2.4	100	0.0047	16	2	4	12	0.455
^{190}Pt	2.49	2.37	3.1	3.2	2.0	2.4	49	0.0038	18	2	6	15	0.538
^{192}Pt	2.48	2.38	3.8	3.8	1.9	2.4	53	0.0021	10	0	8	12	0.698
^{194}Pt	2.47	2.39	3.9	3.9	1.9	2.4	60	0.0023	10	4	5	11	0.688
^{196}Pt	2.47	2.38	3.2	3.1	1.9	2.4	54	0.0043	10	2	6	11	0.676
^{198}Pt	2.42	2.25	2.2	2.3	1.9	2.3	23	0.0059	6	2	4	7	0.372
^{200}Pt	2.35	2.00	2.4	1.9	1.8	2.0	8	0.0000	4	0	4	5	0.342

TABLE II: Comparison of theoretical predictions of the Bohr Hamiltonian with β -dependent mass (with $\delta = \lambda = 0$) for the Kratzer potential for axially symmetric prolate deformed nuclei to experimental data [51] of rare earth and actinides with $R_{4/2} > 2.9$ and known 0_2^+ and 2_1^+ states. The $R_{4/2} = E(4_1^+)/E(2_1^+)$ ratios, as well as the β and γ bandheads, normalized to the 2_1^+ state and labelled by $R_{0/2} = E(0_2^+)/E(2_1^+)$ and $R_{2/2} = E(2_2^+)/E(2_1^+)$ respectively, are shown. The angular momenta of the highest levels of the ground state, β and γ bands included in the rms fit are labelled by L_g , L_β , and L_γ respectively, while n indicates the total number of levels involved in the fit and σ is the quality measure of Eq. (34). The theoretical predictions are obtained from the equations mentioned in Sec. IV. See subsec. VII B for further discussion.

nucleus	$R_{4/2}$ exp	$R_{4/2}$ th	$R_{0/2}$ exp	$R_{0/2}$ th	$R_{2/2}$ exp	$R_{2/2}$ th	\tilde{B}	c	a	L_g	L_β	L_γ	n	σ
^{150}Nd	2.93	3.17	5.2	6.1	8.2	8.5	31	3.3	0.0033	14	6	4	13	0.655
^{152}Sm	3.01	3.22	5.6	5.5	8.9	10.0	48	3.8	0.0050	16	14	9	23	0.622
^{154}Sm	3.25	3.29	13.4	13.6	17.6	18.6	144	6.8	0.0007	16	6	7	17	0.503
^{154}Gd	3.02	3.23	5.5	5.3	8.1	8.4	62	3.0	0.0056	20	20	7	26	0.926
^{156}Gd	3.24	3.29	11.8	11.3	13.0	13.7	159	4.8	0.0014	26	12	16	34	0.973
^{158}Gd	3.29	3.30	15.0	14.8	14.9	15.2	202	5.3	0.0007	12	6	6	14	0.149
^{160}Gd	3.30	3.31	17.6	17.6	13.1	13.0	287	4.4	0.0005	16	4	8	17	0.141
^{162}Gd	3.29	3.31	19.8	19.9	12.0	11.9	261	4.0	0.0002	14	0	4	10	0.097
^{156}Dy	2.93	3.21	4.9	5.1	6.5	6.6	51	2.3	0.0060	20	10	13	27	0.832
^{158}Dy	3.21	3.27	10.0	9.9	9.6	10.1	113	3.5	0.0017	24	8	8	23	0.830
^{160}Dy	3.27	3.29	14.7	14.7	11.1	11.4	176	3.9	0.0006	28	4	23	38	0.927
^{162}Dy	3.29	3.30	17.3	15.5	11.0	11.0	247	3.7	0.0007	18	10	14	27	0.830
^{164}Dy	3.30	3.31	22.6	22.9	10.4	10.2	281	3.4	0.0000	20	0	10	19	0.199
^{166}Dy	3.31	3.30	15.0	15.0	11.2	11.2	214	3.8	0.0007	6	2	5	8	0.060
^{160}Er	3.10	3.24	7.1	7.2	6.8	6.9	65	2.4	0.0031	22	2	5	16	0.874
^{162}Er	3.23	3.27	10.7	10.6	8.8	9.7	100	3.4	0.0012	20	4	12	23	0.518
^{164}Er	3.28	3.29	13.6	12.9	9.4	9.2	179	3.1	0.0010	22	10	19	34	0.915
^{166}Er	3.29	3.29	18.1	17.6	9.8	10.0	167	3.4	0.0000	16	10	14	26	0.340
^{168}Er	3.31	3.31	15.3	14.5	10.3	10.3	384	3.4	0.0010	18	6	8	19	0.274
^{170}Er	3.31	3.32	11.3	9.9	11.9	12.4	491	4.1	0.0018	26	16	19	39	0.807
^{162}Yb	2.92	3.18	3.6	3.6	4.8	5.0	40	1.7	0.0103	20	0	4	13	0.944
^{164}Yb	3.13	3.24	7.9	7.9	7.0	7.2	72	2.5	0.0025	18	0	5	13	0.771
^{166}Yb	3.23	3.28	10.2	9.6	9.1	8.9	138	3.0	0.0020	24	10	13	29	0.974
^{168}Yb	3.27	3.29	13.2	13.0	11.2	11.3	160	3.9	0.0009	24	4	7	20	0.710
^{170}Yb	3.29	3.29	12.7	11.1	13.6	14.0	172	4.9	0.0015	20	18	17	35	0.822
^{172}Yb	3.31	3.31	13.2	12.7	18.6	18.8	246	6.6	0.0012	16	14	5	19	0.787
^{174}Yb	3.31	3.32	19.4	19.1	21.4	21.5	398	7.4	0.0005	20	4	5	16	0.208
^{176}Yb	3.31	3.31	13.9	13.5	15.4	15.5	296	5.3	0.0011	20	2	5	15	0.129
^{178}Yb	3.31	3.31	15.7	15.6	14.5	14.6	254	5.0	0.0007	6	4	2	6	0.025
^{166}Hf	2.97	3.19	4.4	4.4	5.1	5.3	44	1.8	0.0079	20	0	3	12	0.983
^{168}Hf	3.11	3.25	7.6	7.6	7.1	7.6	80	2.6	0.0029	22	4	4	16	1.043
^{170}Hf	3.19	3.27	8.7	8.8	9.5	10.0	99	3.5	0.0022	22	4	4	16	0.928
^{172}Hf	3.25	3.29	9.2	9.0	11.3	11.6	150	4.0	0.0023	26	4	6	20	0.996
^{174}Hf	3.27	3.29	9.1	7.7	13.5	13.9	154	4.9	0.0030	24	20	5	26	1.005
^{176}Hf	3.28	3.30	13.0	12.3	15.2	15.9	190	5.6	0.0012	18	10	8	21	0.569
^{178}Hf	3.29	3.29	12.9	12.9	12.6	13.0	172	4.5	0.0010	18	6	6	17	0.141
^{180}Hf	3.31	3.31	11.8	11.6	12.9	12.8	350	4.3	0.0015	12	4	5	12	0.121
^{176}W	3.22	3.27	7.8	7.3	9.6	10.3	104	3.6	0.0033	22	12	5	21	0.811
^{178}W	3.24	3.27	9.4	8.9	10.5	10.5	97	3.7	0.0021	18	14	2	17	0.356
^{180}W	3.26	3.28	14.6	14.6	10.8	11.4	118	4.0	0.0001	24	0	7	18	0.832
^{182}W	3.29	3.31	11.3	11.5	12.2	12.4	256	4.2	0.0015	18	4	6	16	0.189
^{184}W	3.27	3.29	9.0	9.1	8.1	8.1	164	2.7	0.0023	10	4	6	12	0.091
^{186}W	3.23	3.29	7.2	7.5	6.0	6.1	148	2.0	0.0033	14	4	6	14	0.156
^{176}Os	2.93	3.19	4.5	4.9	6.4	7.0	42	2.5	0.0063	18	6	5	16	0.984
^{178}Os	3.02	3.20	4.9	5.2	6.6	7.2	42	2.6	0.0056	16	6	5	15	0.636
^{180}Os	3.09	3.20	5.6	6.7	6.6	7.4	43	2.7	0.0030	14	4	7	15	0.911
^{184}Os	3.20	3.26	8.7	8.7	7.9	8.4	91	2.9	0.0022	22	0	6	16	0.452
^{186}Os	3.17	3.25	7.7	7.7	5.6	6.0	84	2.0	0.0029	14	10	13	24	0.249
^{188}Os	3.08	3.21	7.0	7.3	4.1	4.3	50	1.4	0.0023	12	2	7	13	0.214
^{190}Os	2.93	3.13	4.9	5.0	3.0	3.1	30	1.0	0.0054	10	2	6	11	0.230

TABLE II: (continued)

nucleus	$R_{4/2}$ exp	$R_{4/2}$ th	$R_{0/2}$ exp	$R_{0/2}$ th	$R_{2/2}$ exp	$R_{2/2}$ th	\tilde{B}	c	a	L_g	L_β	L_γ	n	σ
^{228}Ra	3.21	3.28	11.3	11.1	13.3	13.4	116	4.8	0.0012	22	4	3	15	0.706
^{228}Th	3.24	3.28	14.4	14.2	16.8	17.1	120	6.3	0.0003	18	2	5	14	0.396
^{230}Th	3.27	3.30	11.9	11.7	14.7	14.7	213	5.1	0.0014	24	4	4	17	0.625
^{232}Th	3.28	3.31	14.8	14.5	15.9	16.0	268	5.5	0.0009	30	20	12	36	0.964
^{232}U	3.29	3.30	14.5	14.8	18.2	18.2	234	6.4	0.0008	20	10	4	18	0.244
^{234}U	3.30	3.31	18.6	19.1	21.3	21.4	307	7.5	0.0004	28	8	7	24	0.785
^{236}U	3.30	3.31	20.3	19.8	21.2	21.3	354	7.4	0.0004	30	4	5	21	0.700
^{238}U	3.30	3.31	20.6	20.2	23.6	24.4	378	8.5	0.0004	30	4	27	43	0.911
^{238}Pu	3.31	3.32	21.4	21.5	23.3	23.3	498	8.0	0.0004	26	2	4	17	0.368
^{240}Pu	3.31	3.32	20.1	19.6	26.6	26.7	452	9.3	0.0005	26	4	4	18	0.516
^{242}Pu	3.31	3.32	21.5	20.8	24.7	24.8	422	8.6	0.0004	26	2	2	15	0.402
^{248}Cm	3.31	3.32	25.0	24.3	24.2	24.2	429	8.4	0.0002	28	4	2	17	0.458
^{250}Cf	3.32	3.31	27.0	27.0	24.2	24.1	375	8.4	0.0000	8	2	4	8	0.078

TABLE III: Normalized [to the energy of the first excited state, $E(2_1^+)$] energy levels of the ground state band (gsb) and the β_1 and γ_1 bands of ^{170}Er and ^{232}Th , obtained from the Bohr Hamiltonian with β -dependent mass for the Kratzer potential for axially symmetric prolate deformed nuclei using the parameters given in Table II, compared to experimental data [51]. See subsec. VII B for further discussion.

^{170}Er		^{170}Er		^{232}Th		^{232}Th		^{170}Er		^{170}Er		^{232}Th		^{232}Th	
L	exp	th	exp	th	exp	th	exp	th	L	exp	th	exp	th	exp	th
	gsb	gsb	gsb	gsb	β_1	β_1	β_1	β_1		γ_1	γ_1	γ_1	γ_1		
0	0.00	0.00	0.00	0.00	11.3	9.9	14.8	14.5	2	11.9	12.4	15.9	16.0		
2	1.00	1.00	1.00	1.00	12.2	10.8	15.7	15.4	3	12.9	13.3	16.8	16.9		
4	3.31	3.32	3.28	3.31	14.0	13.0	17.7	17.5	4	14.3	14.6	18.0	18.0		
6	6.88	6.92	6.75	6.86	17.2	16.3	20.7	20.7	5	15.7	16.1	19.5	19.5		
8	11.64	11.75	11.28	11.56	21.3	20.8	24.8	24.9	6	17.8	18.0	21.3	21.2		
10	17.51	17.73	16.75	17.31	26.5	26.4	29.8	30.1	7	19.8	20.2	23.2	23.2		
12	24.41	24.79	23.03	23.95	32.5	33.0	35.5	36.1	8	22.6	22.6	25.5	25.5		
14	32.28	32.82	30.04	31.35	39.1	40.5	42.1	42.8	9	25.0	25.4	27.8	28.0		
16	41.04	41.73	37.65	39.35	46.2	48.8	49.4	50.1	10	28.3	28.4	30.6	30.7		
18	50.62	51.39	45.84	47.82			57.4	57.8	11	31.1	31.6	33.2	33.6		
20	60.91	61.70	55.52	56.61			65.8	65.8	12	35.8	35.1	36.5	36.7		
22	72.20	72.55	63.69	65.60					13	39.1	38.9				
24	83.80	83.82	73.32	74.67					14	43.7	42.8				
26	95.82	95.42	83.38	83.73					15	47.2	47.0				
28			93.82	92.69					16	52.6	51.4				
30			104.56	101.49					17	56.2	55.9				
									18	62.2	60.6				
									19	66.2	65.5				

TABLE IV: Normalized [to the energy of the first excited state, $E(2_1^+)$] energy levels of the ground state band (gsb) and the β_1 and γ_1 bands of the $N = 90$ isotones ^{150}Nd , ^{152}Sm , ^{154}Gd , and ^{156}Dy , obtained from the Bohr Hamiltonian with β -dependent mass for the Kratzer potential for axially symmetric prolate deformed nuclei using the parameters given in Table II, compared to experimental data [51] and to the predictions of the X(5) critical point symmetry [36, 55, 56]. The bandhead of the γ_1 band in X(5), which is a free parameter, has been set equal to the average of the relevant experimental values. See subsec. VII B for further discussion.

	^{150}Nd	^{150}Nd	^{152}Sm	^{152}Sm	^{154}Gd	^{154}Gd	^{156}Dy	^{156}Dy	X(5)
L	exp	th	exp	th	exp	th	exp	th	
gsb									
0	0.00	0.00	0.00	0.00	0.00	0.00	0.00	0.00	0.00
2	1.00	1.00	1.00	1.00	1.00	1.00	1.00	1.00	1.00
4	2.93	3.17	3.01	3.22	3.02	3.23	2.93	3.21	2.90
6	5.53	6.18	5.80	6.40	5.83	6.49	5.59	6.39	5.43
8	8.68	9.64	9.24	10.24	9.30	10.48	8.82	10.20	8.48
10	12.28	13.24	13.21	14.43	13.30	14.92	12.52	14.35	12.03
12	16.27	16.72	17.64	18.70	17.75	19.56	16.59	18.58	16.04
14	20.60	19.95	22.47	22.87	22.57	24.18	20.96	22.68	20.51
16			27.61	26.81	27.66	28.63	25.57	26.55	25.44
18					33.21	32.83	30.33	30.11	30.80
20					38.86	36.71	35.27	33.34	36.61
β_1									
0	5.2	6.1	5.6	5.5	5.5	5.3	4.9	5.1	5.6
2	6.5	6.9	6.7	6.3	6.6	6.1	6.0	5.9	7.5
4	8.7	8.5	8.4	8.1	8.5	8.0	7.9	7.7	10.7
6	11.8	10.9	10.8	10.7	11.1	10.7	10.4	10.3	14.8
8			13.7	13.9	14.3	14.0	13.5	13.5	19.4
10			17.1	17.4	17.8	17.8	16.8	16.9	24.7
12			20.7	21.0	21.3	21.7			30.5
14			24.4	24.5	24.6	25.7			36.7
16					28.4	29.6			43.5
18					32.6	33.3			50.7
20					37.8	36.7			58.4
γ_1									
2	8.2	8.5	8.9	10.0	8.1	8.4	6.5	6.6	7.9
3	9.2	9.2	10.1	10.8	9.2	9.2	7.4	7.4	8.9
4	10.4	10.0	11.3	11.7	10.3	10.2	8.5	8.4	9.9
5			12.8	12.8	11.6	11.5	9.7	9.7	11.2
6			14.2	14.1	13.1	12.9	11.1	11.1	12.5
7			16.0	15.5	14.7	14.5	12.5	12.6	14.0
8			17.6	17.0			14.2	14.3	15.6
9			19.5	18.6			15.9	16.0	17.4
10							17.8	17.8	19.2
11							19.7	19.7	21.2
12							21.8	21.5	23.3
13							23.8	23.3	25.4

TABLE V: Comparison of experimental data [51] (upper line) for several $B(E2)$ ratios of γ -unstable nuclei to predictions (lower line) by the Bohr Hamiltonian with β -dependent mass (with $\delta = \lambda = 0$) for the Kratzer potential, for the parameter values shown in Table I. See subsec. VII C for further discussion.

nucl.	$\frac{4_1 \rightarrow 2_1}{2_1 \rightarrow 0_1}$	$\frac{6_1 \rightarrow 4_1}{2_1 \rightarrow 0_1}$	$\frac{8_1 \rightarrow 6_1}{2_1 \rightarrow 0_1}$	$\frac{10_1 \rightarrow 8_1}{2_1 \rightarrow 0_1}$	$\frac{2_2 \rightarrow 2_1}{2_1 \rightarrow 0_1}$	$\frac{2_2 \rightarrow 0_1}{2_1 \rightarrow 0_1}$ x 10^3	$\frac{0_2 \rightarrow 2_1}{2_1 \rightarrow 0_1}$	$\frac{2_3 \rightarrow 0_1}{2_1 \rightarrow 0_1}$ x 10^3
⁹⁸ Ru	1.44(25)				1.62(61)	36.0(152)		
	1.77	2.81	4.63	8.42	1.77	0.0	1.27	27.84
¹⁰⁰ Ru	1.45(13)				0.64(12)	41.1(52)	0.98(15)	
	1.70	2.56	3.93	6.59	1.70	0.0	1.11	43.07
¹⁰² Ru	1.50(24)				0.62(7)	24.8(7)	0.80(14)	
	1.77	2.82	4.68	8.67	1.77	0.0	1.29	31.06
¹⁰⁴ Ru	1.18(28)				0.63(15)	35.0(84)	0.42(7)	
	1.60	2.20	2.95	4.00	1.60	0.0	0.68	25.59
¹⁰² Pd	1.56(19)				0.46(9)	128.8(735)		
	1.63	2.31	3.25	4.77	1.63	0.0	0.87	41.64
¹⁰⁴ Pd	1.36(27)				0.61(8)	33.3(74)		
	1.70	2.52	3.74	5.83	1.70	0.0	0.99	24.16
¹⁰⁶ Pd	1.63(28)				0.98(12)	26.2(31)	0.67(18)	
	1.74	2.66	4.13	6.83	1.74	0.0	1.12	22.91
¹⁰⁸ Pd	1.47(20)	2.16(28)	2.99(48)		1.43(14)	16.6(18)	1.05(13)	1.90(29)
	1.66	2.38	3.42	5.11	1.66	0.0	0.89	30.31
¹¹⁰ Pd	1.71(34)				0.98(24)	14.1(22)	0.64(10)	
	1.60	2.18	2.94	4.06	1.60	0.0	0.75	42.18
¹⁰⁶ Cd	1.78(25)				0.43(12)	93.0(127)		
	1.66	2.37	3.34	4.76	1.66	0.0	0.83	16.97
¹⁰⁸ Cd	1.54(24)				0.64(20)	67.7(120)		
	1.67	2.40	3.43	5.01	1.67	0.0	0.87	19.88
¹¹⁰ Cd	1.68(24)				1.09(19)	48.9(78)		9.85(595)
	1.85	3.14	5.63	11.54	1.85	0.0	1.52	20.99
¹¹² Cd	2.02(22)				0.50(10)	19.9(35)	1.69(48)	11.26(210)
	1.95	3.53	6.92	15.92	1.95	0.0	1.82	12.87
¹¹⁴ Cd	1.99(25)	3.83(72)	2.73(97)		0.71(24)	15.4(29)	0.88(11)	10.61(193)
	1.93	3.46	6.72	15.44	1.93	0.0	1.77	15.44
¹¹⁶ Cd	1.70(52)				0.63(46)	32.8(86)	0.02	
	1.69	2.47	3.52	5.05	1.69	0.0	0.90	10.02
¹¹⁸ Cd	>1.85						0.16(4)	
	1.70	2.51	3.65	5.41	1.70	0.0	0.95	13.14
¹¹⁸ Xe	1.11(7)	0.88(27)	0.49(20)	>0.73				
	1.61	2.21	3.00	4.17	1.61	0.0	0.74	34.42
¹²⁰ Xe	1.16(14)	1.17(24)	0.96(22)	0.91(19)				
	1.56	2.06	2.64	3.43	1.56	0.0	0.62	42.25
¹²² Xe	1.47(38)	0.89(26)	>0.44					
	1.54	2.00	2.52	3.17	1.54	0.0	0.54	36.27
¹²⁴ Xe	1.34(24)	1.59(71)	0.63(29)	0.29(8)	0.70(19)	15.9(46)		
	1.55	2.03	2.57	3.25	1.55	0.0	0.53	28.40
¹²⁸ Xe	1.47(20)	1.94(26)	2.39(40)	2.74(114)	1.19(19)	15.9(23)		
	1.83	2.95	4.73	7.64	1.83	0.0	0.75	12.57
¹³² Xe	1.24(18)				1.77(29)	3.4(7)		
	2.78	7.13	17.89	43.35	2.78	0.0	2.49	0.07
¹³⁰ Ba	1.36(6)	1.62(15)	1.55(56)	0.93(15)				
	1.54	2.01	2.54	3.22	1.54	0.0	0.56	39.43
¹³² Ba					3.35(64)	90.7(177)		
	1.61	2.20	2.94	3.95	1.61	0.0	0.66	20.59
¹³⁴ Ba	1.55(21)				2.17(69)	12.5(41)		
	2.13	4.10	7.88	15.19	2.13	0.0	1.26	6.22
¹⁴² Ba	1.40(17)	0.56(14)						
	1.54	1.99	2.46	3.04	1.54	0.0	0.45	21.34
¹⁴⁸ Nd	1.61(13)	1.76(19)			0.25(4)	9.3(17)	0.54(6)	32.82(816)
	1.57	2.08	2.67	3.47	1.57	0.0	0.59	30.88

TABLE V: (continued)

nucl.	$\frac{4_1 \rightarrow 2_1}{2_1 \rightarrow 0_1}$	$\frac{6_1 \rightarrow 4_1}{2_1 \rightarrow 0_1}$	$\frac{8_1 \rightarrow 6_1}{2_1 \rightarrow 0_1}$	$\frac{10_1 \rightarrow 8_1}{2_1 \rightarrow 0_1}$	$\frac{2_2 \rightarrow 2_1}{2_1 \rightarrow 0_1}$	$\frac{2_2 \rightarrow 0_1}{2_1 \rightarrow 0_1}$ x 10^3	$\frac{0_2 \rightarrow 2_1}{2_1 \rightarrow 0_1}$	$\frac{2_3 \rightarrow 0_1}{2_1 \rightarrow 0_1}$ x 10^3
^{152}Gd	1.84(29)	2.74(81)			0.23(4)	4.2(8)	2.47(78)	
	1.80	2.96	5.14	10.30	1.80	0.0	1.41	32.70
^{154}Dy	1.62(35)	2.05(42)	2.27(62)	1.86(69)				
	1.78	2.89	5.06	10.73	1.78	0.0	1.46	58.09
^{156}Er	1.78(16)	1.89(36)	0.76(20)	0.88(22)				
	1.64	2.33	3.27	4.73	1.64	0.0	0.83	28.76
^{192}Pt	1.56(12)	1.23(55)			1.91(16)	9.5(9)		
	1.57	2.09	2.68	3.44	1.57	0.0	0.54	17.79
^{194}Pt	1.73(13)	1.36(45)	1.02(30)	0.69(19)	1.81(25)	5.9(9)	0.01	
	1.56	2.07	2.63	3.34	1.56	0.0	0.52	19.45
^{196}Pt	1.48(3)	1.80(23)	1.92(23)			0.4	0.07(4)	0.06(6)
	1.61	2.21	2.97	4.04	1.61	0.0	0.69	23.11
^{198}Pt	1.19(13)	>1.78			1.16(23)	1.2(4)	0.81(22)	1.56(126)
	1.76	2.73	4.24	6.76	1.76	0.0	1.16	11.09

TABLE VI: Comparison of experimental data [51] (upper line) for several $B(E2)$ ratios of axially symmetric prolate deformed nuclei to predictions (lower line) by the Bohr Hamiltonian with β -dependent mass (with $\delta = \lambda = 0$) for the Kratzer potential, for the parameter values shown in Table II. In order to facilitate comparisons of the $N = 90$ isotones ^{150}Nd , ^{152}Sm , ^{154}Gd , and ^{156}Dy , to the predictions of the X(5) critical point symmetry [36, 55, 56], the relevant predictions are reported in the first line of the table, with the $\gamma_1 \rightarrow gsb$ transitions normalized to the $2_\gamma \rightarrow 0_1$ transition, which is set equal to 100, close to the average value for the first three $N = 90$ isotones. See subsec. VIID for further discussion.

nucl.	$\frac{4_1 \rightarrow 2_1}{2_1 \rightarrow 0_1}$	$\frac{6_1 \rightarrow 4_1}{2_1 \rightarrow 0_1}$	$\frac{8_1 \rightarrow 6_1}{2_1 \rightarrow 0_1}$	$\frac{10_1 \rightarrow 8_1}{2_1 \rightarrow 0_1}$	$\frac{2_\beta \rightarrow 0_1}{2_1 \rightarrow 0_1}$ x 10^3	$\frac{2_\beta \rightarrow 2_1}{2_1 \rightarrow 0_1}$ x 10^3	$\frac{2_\beta \rightarrow 4_1}{2_1 \rightarrow 0_1}$ x 10^3	$\frac{2_\gamma \rightarrow 0_1}{2_1 \rightarrow 0_1}$ x 10^3	$\frac{2_\gamma \rightarrow 2_1}{2_1 \rightarrow 0_1}$ x 10^3	$\frac{2_\gamma \rightarrow 4_1}{2_1 \rightarrow 0_1}$ x 10^3
X(5)	1.60	1.98	2.28	2.51	21.2	82.2	366	100.0	150.0	7.8
^{150}Nd	1.52(4)	1.84(14)	2.05(13)		4.4(8)	61.7(98)	174(55)	26.1(22)	49.6(26)	14.8(98)
	1.55	1.98	2.55	3.40	36.4	93.5	443	95.9	150.0	9.0
^{152}Sm	1.45(5)	1.70(7)	1.98(14)	2.22(25)	6.4(7)	38.2(43)	132(15)	25.1(17)	64.6(48)	5.4(5)
	1.55	1.98	2.58	3.53	49.1	113.4	475	84.0	130.9	7.8
^{154}Sm	1.40(5)	1.67(7)	1.83(11)	1.81(11)	5.4(13)		25(6)	18.4(34)		3.9(7)
	1.46	1.67	1.86	2.05	24.7	45.7	136	47.8	69.9	3.7
^{154}Gd	1.56(7)	1.82(11)	1.99(12)	2.29(27)	5.5(5)	42.7(41)	125(11)	36.3(34)	78.3(69)	11.0(10)
	1.55	1.98	2.57	3.54	55.4	122.5	486	114.7	175.6	10.1
^{156}Gd	1.41(5)	1.58(6)	1.71(10)	1.68(9)	3.4(3)	18(2)	22(2)	25.0(15)	38.7(24)	4.1(3)
	1.47	1.69	1.90	2.13	30.8	56.5	166	70.7	103.3	5.4
^{158}Gd	1.46(5)		1.67(16)	1.72(16)	1.6(2)	0.4(1)	7.0(8)	17.2(20)	30.3(45)	1.4(2)
	1.45	1.66	1.82	1.98	24.1	42.8	119	63.9	92.6	4.8
^{156}Dy	1.75(14)	1.34(12)	1.94(13)	2.45(21)				48.2(35)	63.0(78)	84.4(141)
	1.56	2.03	2.70	3.83	53.2	124.3	531	151.8	232.6	13.4
^{158}Dy	1.45(10)	1.86(12)	1.86(38)	1.75(28)	12(3)	19(4)	66(16)	32.2(78)	103.8(258)	11.5(48)
	1.48	1.73	1.98	2.28	32.5	63.0	202	97.9	143.6	7.6
^{160}Dy	1.46(7)	1.23(7)	1.70(16)	1.69(9)	3.4(4)		8.5(10)	23.2(21)	43.8(42)	3.1(3)
	1.46	1.66	1.83	2.00	23.5	42.5	122	87.4	126.6	6.5
^{162}Dy	1.45(7)	1.51(10)	1.74(10)	1.76(13)				0.12(1)	0.20	0.02
	1.45	1.65	1.80	1.95	23.7	41.4	112	92.3	133.2	6.8
^{164}Dy	1.30(7)	1.56(7)	1.48(9)	1.69(9)				19.1(22)	38.3(39)	4.6(5)
	1.45	1.64	1.79	1.93	23.6	40.6	107	100.4	144.7	7.4
^{162}Er				8(7)			170(90)	32.5(28)	77.0(56)	9.4(69)
	1.48	1.73	1.97	2.25	28.9	57.1	189	100.4	147.1	7.8
^{164}Er	1.18(13)		1.57(9)	1.64(11)				23.9(35)	52.3(72)	7.8(12)
	1.46	1.67	1.86	2.05	27.0	49.0	141	110.5	160.2	8.2
^{166}Er	1.45(12)	1.62(22)	1.71(25)	1.73(23)				25.7(31)	45.3(54)	3.1(4)
	1.48	1.74	2.00	2.31	21.2	39.2	117			
^{168}Er	1.54(7)	2.13(16)	1.69(11)	1.46(11)				23.2(15)	41.1(31)	3.0(3)
	1.45	1.64	1.78	1.92	27.6	46.2	116	100.6	144.9	7.4
^{170}Er			1.78(15)	1.54(11)	1.4(1)	0.2(2)	6.8(12)	17.7(9)		1.4(4)
	1.46	1.66	1.83	2.01	42.8	70.7	173	84.6	122.2	6.3
^{166}Yb	1.43(9)	1.53(10)	1.70(18)	1.61(80)						
	1.48	1.73	1.97	2.27	35.4	66.7	206	115.2	168.2	8.8
^{168}Yb				8.6(9)				22.0(55)	45.9(73)	8.6
	1.46	1.68	1.86	2.06	26.3	48.2	142	87.6	127.2	6.6
^{170}Yb			1.79(16)	1.77(14)	5.4(10)			13.4(34)	23.9(57)	2.4(6)
	1.47	1.69	1.90	2.13	31.9	58.0	168	69.4	101.3	5.3
^{172}Yb	1.42(10)	1.51(14)	1.89(19)	1.77(11)	1.1(1)	3.7(6)	12(1)	6.3(6)		0.6(1)
	1.46	1.66	1.83	2.01	29.6	51.6	139	51.0	74.2	3.8
^{174}Yb	1.39(7)	1.84(26)	1.93(12)	1.67(12)					12.4(29)	
	1.44	1.62	1.74	1.86	20.6	34.3	85	45.7	65.8	3.4
^{176}Yb	1.49(15)	1.63(14)	1.65(28)	1.76(18)				9.8		
	1.45	1.65	1.81	1.97	28.6	49.0	128	64.5	93.4	4.8

TABLE VI: (continued)

nucl.	$\frac{4_1 \rightarrow 2_1}{2_1 \rightarrow 0_1}$	$\frac{6_1 \rightarrow 4_1}{2_1 \rightarrow 0_1}$	$\frac{8_1 \rightarrow 6_1}{2_1 \rightarrow 0_1}$	$\frac{10_1 \rightarrow 8_1}{2_1 \rightarrow 0_1}$	$\frac{2_\beta \rightarrow 0_1}{2_1 \rightarrow 0_1}$ x 10^3	$\frac{2_\beta \rightarrow 2_1}{2_1 \rightarrow 0_1}$ x 10^3	$\frac{2_\beta \rightarrow 4_1}{2_1 \rightarrow 0_1}$ x 10^3	$\frac{2_\gamma \rightarrow 0_1}{2_1 \rightarrow 0_1}$ x 10^3	$\frac{2_\gamma \rightarrow 2_1}{2_1 \rightarrow 0_1}$ x 10^3	$\frac{2_\gamma \rightarrow 4_1}{2_1 \rightarrow 0_1}$ x 10^3
^{174}Hf					14(4)		9(3)	31.6(161)	48.7(124)	
	1.49	1.76	2.05	2.42	47.1	87.5	264	69.7	102.9	5.5
^{176}Hf					5.4(11)		31(6)	21.3(26)		
	1.46	1.68	1.86	2.06	29.1	52.2	148	60.3	87.8	4.6
^{178}Hf		1.38(9)	1.49(6)	1.62(7)	0.4(2)		2.4(9)	24.5(39)	27.7(28)	1.6(2)
	1.46	1.68	1.86	2.06	27.1	49.2	142	75.7	110.0	5.7
^{180}Hf	1.48(20)	1.41(15)	1.61(26)	1.55(10)				24.5(47)	32.9(56)	
	1.46	1.66	1.83	2.00	34.6	58.6	150	80.3	116.0	6.0
^{182}W	1.43(8)	1.46(16)	1.53(14)	1.48(14)	6.6(6)	4.6(6)	13(1)	24.8(12)	49.2(24)	0.2
	1.46	1.67	1.85	2.05	33.0	57.5	155	82.0	118.9	6.1
^{184}W	1.35(12)	1.54(9)	2.00(18)	2.45(51)	1.8(3)		24(3)	37.1(28)	70.6(51)	4.0(4)
	1.48	1.73	1.97	2.27	38.9	71.8	214	128.4	187.1	9.8
^{186}W	1.30(9)	1.69(12)	1.60(12)	1.36(36)				41.7(92)	91.0(201)	
	1.49	1.77	2.08	2.48	47.3	89.1	275	174.0	254.4	13.3
^{186}Os	1.45(7)	1.99(7)	1.89(11)	2.06(44)				109.4(71)	254.6(150)	13.0(47)
	1.50	1.81	2.16	2.63	39.2	81.0	288	173.5	255.9	13.6
^{188}Os	1.68(11)	1.75(11)	2.04(15)	2.38(32)				63.3(92)	202.5(304)	43.0(74)
	1.52	1.87	2.29	2.87	33.6	78.5	330	246.6	366.2	19.7
^{230}Th	1.36(8)				5.7(26)		20(11)	15.6(59)	28.1(100)	1.8(11)
	1.46	1.68	1.86	2.07	31.4	55.6	155	66.9	97.3	5.1
^{232}Th	1.44(15)	1.65(14)	1.73(12)	1.82(15)	14(6)	2.6(13)	17(8)	14.6(28)	36.4(56)	0.7
	1.45	1.65	1.80	1.96	26.0	44.9	119	61.9	89.6	4.6
^{234}U								12.5(27)	21.1(44)	1.2(3)
	1.45	1.63	1.76	1.88	19.9	33.8	87	44.7	64.5	3.3
^{236}U	1.42(11)	1.55(11)	1.59(17)	1.46(17)						
	1.44	1.62	1.75	1.86	19.5	32.7	82	45.5	65.6	3.3
^{238}U			1.45(23)	1.71(22)	1.4(6)	3.6(14)	12(5)	10.8(8)	18.9(17)	1.2(1)
	1.44	1.62	1.74	1.85	19.3	32.3	80	39.4	56.8	2.9
^{238}Pu					14(4)		11(4)			
	1.44	1.61	1.73	1.82	18.8	30.8	74	42.2	60.7	3.1
^{250}Cf								6.8(17)	10.9(25)	0.6(1)
	1.45	1.65	1.80	1.96	15.5	26.1	66			

TABLE VII: Numerical values of the rescaling parameter A for the γ -unstable nuclei shown in Figs. 2 and 3. β_0 is the position of the minimum of the effective potential, calculated using in Eq. (129) the parameter values given in Table I, β_{exp} is the value of the quadrupole deformation taken from the experimental value of $B(E2; 0_1 \rightarrow 2_1)$ [61], while A is calculated from Eq. (130).

nucleus	β_0	β_{exp}	$10^3 A$
^{126}Xe	123.73	0.1881	1.520
^{128}Xe	66.00	0.1836	2.782
^{130}Xe	60.17	0.169	2.809
^{132}Xe	20.00	0.1409	7.045
^{134}Xe	12.00	0.119	9.917
^{130}Ba	286.86	0.2183	0.761
^{132}Ba	103.53	0.186	1.797
^{134}Ba	38.00	0.1609	4.234
^{136}Ba	18.01	0.1258	6.983

TABLE VIII: Numerical values of the rescaling parameter A for the prolate deformed nuclei shown in Figs. 4, 5 and 6. β_0 is the position of the minimum of the effective potential, calculated using in Eq. (131) the parameter values given in Table II, β_{exp} is the value of the quadrupole deformation taken from the experimental value of $B(E2; 0_1 \rightarrow 2_1)$ [61], while A is calculated from Eq. (132).

nucleus	β_0	β_{exp}	$10^3 A$
^{150}Nd	90.94	0.2853	3.137
^{152}Sm	139.49	0.3064	2.197
^{154}Gd	164.23	0.3120	1.900
^{156}Gd	365.59	0.3378	0.924
^{158}Gd	449.05	0.3484	0.776
^{160}Gd	611.70	0.3534	0.578
^{156}Dy	131.89	0.2929	2.221
^{158}Dy	260.05	0.3255	1.252
^{160}Dy	383.71	0.3387	0.883
^{162}Dy	527.88	0.3430	0.650
^{164}Dy	584.40	0.3481	0.596